

**Screening Glycolipids Against Proteins in vitro using Picodiscs and
Catch-and-Release Electrospray Ionization Mass Spectrometry**

Jun Li,^{1,2} Xuxin Fan,^{1,2} Elena N. Kitova,^{1,2} Chunxia Zou,^{1,2} Christopher W. Cairo,^{1,2} Luiz
Eugenio,^{1,3} Kenneth K. S. Ng,^{1,3} Zi Jian Xiong,⁴ Gilbert G. Privé,^{4,5} John S. Klassen^{1,2*}

¹*Alberta Glycomics Centre*

²*Department of Chemistry, University of Alberta, Edmonton, Alberta, Canada T6G 2G2*

³*Department of Biological Sciences, University of Calgary, Calgary, Alberta, Canada T2N 1N4*

⁴*Department of Biochemistry, University of Toronto, Toronto, Ontario, Canada M5S 1A8*

⁵*Princess Margaret Cancer Centre, University Health Network, Toronto, Ontario, Canada*

M5G 1L7

*Email: john.klassen@ualberta.ca

Abstract

This work describes the application of the catch-and-release electrospray ionization mass spectrometry (CaR-ESI-MS) assay, implemented using picodiscs (complexes comprised of saposin A and lipids, PDs), to screen mixtures of glycolipids (GLs) against water-soluble proteins to detect specific interactions. To demonstrate the reliability of the method, seven gangliosides (GM1, GM2, GM3, GD1a, GD1b, GD2 and GT1b) were incorporated, either individually or as a mixture, into PDs and screened against two lectins: the B subunit homopentamer of cholera toxin (CTB₅) and a sub-fragment of toxin A from *Clostridium difficile* (TcdA-A2). The CaR-ESI-MS results revealed that CTB₅ binds to six of the gangliosides (GM1, GM2, GM3, GD1a, GD1b and GT1b), while TcdA-A2 binds to five of them (GM1, GM2, GM3, GD1a and GT1b). These findings are consistent with the measured binding specificities of these proteins for ganglioside oligosaccharides. Screening mixtures of lipids extracted from porcine brain and a human epithelial cell line against CTB₅ revealed binding to multiple GM1 isoforms, as well as to fucosyl-GM1, which is a known ligand. Finally, a comparison of the present results with data obtained with the CaR-ESI-MS assay implemented using nanodiscs (NDs) revealed that the PDs exhibited similar or superior performance to NDs for protein-GL binding measurements.

Introduction

The interactions between proteins and glycolipids (GLs), which consist of a mono-, oligo- or polysaccharides covalently attached to a lipid moiety, represent an important class of cellular recognition processes.¹⁻⁴ Despite their importance in normal and pathological cellular processes, the identification and characterization of protein-GL interactions remains challenging and new experimental techniques are needed.⁵⁻⁶ The key challenges to the detection and characterization of protein-GLs complexes are the relative insolubility of the GLs in water, which imposes limitations on how the binding measurements are performed; the low affinities characteristic of monovalent protein-carbohydrate interactions, which require sensitive detection methods and the expected dependence of the properties of the interactions on the nature of the lipid environment.⁷⁻⁹ Commonly used methods for detecting protein-GL binding, such as thin layer chromatography (TLC) overlay, enzyme-linked immunosorbent assays (ELISA) and surface plasmon resonance (SPR) spectroscopy, employ GLs immobilized on a solid surface.⁵ While convenient, such a presentation of GLs differs significantly from the native lipid environment of cell membranes. The incorporation of GLs into model membranes (*e.g.* micelles, bicelles, liposomes and nanodiscs (NDs)) allows for a more physiological presentation of GLs and the possibility of probing the influence of the lipid environment on binding. Increasingly conventional binding assays, including electrospray ionization-mass spectrometry (ESI-MS), are being adapted for use with model membranes to allow for protein-GL interaction studies to be carried out in a membrane-like environment.¹⁰⁻¹³

Recently protein interactions with gangliosides (sialic acid containing glycosphingolipids) were detected using the catch-and-release (CaR)-ESI-MS assay implemented with NDs.¹⁰⁻¹¹ Briefly, the assay involves transferring the protein-GL-ND complexes, which are present in solution, to the gas phase using ESI. Intact protein-GL

complexes are released from the NDs in the ion source, isolated and then subjected to collision-induced dissociation (CID) to release the GL ligands for identification purposes. Both neutral and acidic GLs are readily incorporated into NDs, which are ~150 kDa water-soluble discoidal phospholipid bilayers surrounded by two copies of an amphipathic membrane scaffold protein (MSP), thereby allowing their interactions with water-soluble proteins to be investigated.^{10-11,14} Because of their size, each ND can accommodate a significant number of GLs (NDs containing up to thirty gangliosides have been reported) and allow for binding studies to be carried out using a wide range of lipid compositions.¹¹⁻¹² Moreover, NDs can serve as GL arrays and can be combined with the CaR-ESI-MS assay to rapidly screen known and unknown mixtures of GLs against target proteins.¹¹ However, the use of NDs has several drawbacks, such as their tendency to disassemble in aqueous solution at room temperature and the inherent challenges in accurately characterizing their lipid composition. More recently, the implementation of the CaR-ESI-MS assay with lipid-transporting macromolecular complexes called picodiscs (PDs) to detect both high and low affinity protein–GL interactions was described.¹³ Picodiscs are reported to be composed of two copies of the human sphingolipid activator protein saposin A (SapA) and a small number (8-12) of phospholipids.¹⁵ Picodiscs containing GLs have been shown to have advantages over NDs for the detection of some protein–GL interactions and for studying the kinetics of GL-processing enzymes.¹³ Furthermore, PDs are stable at room temperature for periods of weeks¹³ and, therefore, are attractive as GL arrays for *in vitro* screening.

The goal of the present study was to investigate the feasibility of implementing the CaR-ESI-MS assay with PDs to screen libraries of GLs against water-soluble proteins. The B subunit homopentamer of cholera toxin (CTB₅) and a sub-fragment of toxin A (TcdA-A2) from *Clostridium difficile* (TcdA), served as model GL-binding proteins for this work. The CTB

subunits, each possessing a single, dominant, carbohydrate binding site, are responsible for cellular recognition.¹⁶ The interactions between CTB₅ with its native receptor GM1, as well as other gangliosides and their corresponding oligosaccharides, have been extensively studied.¹⁷⁻¹⁸ The apparent association constants (K_a) for the stepwise binding of the GM1 pentasaccharide (β -D-Gal-(1→3)- β -D-GalNAc-(1→4)-[α -D-Neu5Ac-(2→3)]- β -D-Gal-(1→4)-D-Glc, Figure S1, Supporting Information) to CTB₅ range from 2×10^6 to 2×10^7 M⁻¹.¹⁹ Binding of CTB₅ to other ganglioside oligosaccharides is suggested to be much weaker, although quantitative binding data have not been reported.¹⁸ The exotoxin TcdA, which is one of the main virulence factors of *C. difficile*, consists of four regions: a N-terminal domain which is responsible for the glucosylating activity of the toxin, a cysteine protease domain, a delivery/pore forming domain, and a C-terminal domain containing combined repetitive oligopeptides, which is responsible for receptor binding on target cell surfaces.²⁰⁻²¹ Although the functional human receptors of TcdA have not been conclusively identified, it is known that TcdA binds to a variety of carbohydrate structures, including the trisaccharide α -D-Gal-(1→3)- β -D-Gal-(1→4)-D-GlcNAc,²² several Lewis X, Y and I glycan sequences,²³⁻²⁴ the glycosphingolipid β -D-GalNAc-(1→3)- β -D-Gal-(1→4)- β -D-GlcNAc-(1→3)- β -D-Gal-(1→4)- β -D-Glc-cer²⁵⁻²⁶ and several ganglioside oligosaccharides (*e.g.* GM1_{aos}, GM2_{os}, GM3_{os}, GT1b_{os}, GD3_{os}, GD1a_{os}, GT3_{os}, GT1a_{os}, GT1b_{os}).²⁷ In the present study, the CaR-ESI-MS assay was used to screen a small library of gangliosides (GM1, GM2, GM3, GD1a, GD1b, GD2 and GT1b) against CTB₅ and TcdA-A2; the screening results were validated using binding data measured for the corresponding ganglioside oligosaccharides. The assay was also used to screen mixtures of GLs extracted from porcine brain, as well as a human epithelial cell line, against CTB₅ to demonstrate the applicability of the assay for analysis of natural GL libraries.

Experimental Section

Proteins

Cholera toxin B subunit homopentamer from *Vibrio cholerae* (CTB₅, homopentamer molecular weight (MW) 58,020 Da) was purchased from Sigma-Aldrich Canada (Oakville, Canada). The A2 subfragment of *Clostridium difficile* toxin (TcdA-A2, MW 29,575 Da) and the single chain variable fragment (scFv, MW 26,539 Da) of the monoclonal antibody (mAb) Se155-4 were expressed in *Escherichia coli* and purified as described previously.²⁸⁻²⁹ Saposin A (SapA, two major isoforms with MWs 8,918 Da and MW 9,049 Da) and recombinant MSP (MSP1E1, MW 27,494 Da) were expressed and purified as previously described.¹⁴⁻¹⁵ Shiga toxin type 1 B subunit homopentamer (Stx1B₅, MW 38,455 Da) was a gift from Prof. G. Armstrong (University of Calgary).

Lipids and Glycolipids

The gangliosides β -D-Gal-(1 \rightarrow 3)- β -D-GalNAc-(1 \rightarrow 4)-[α -D-Neu5Ac-(2 \rightarrow 3)]- β -D-Gal-(1 \rightarrow 4)-D-Glc-ceramide (GM1, major isoforms *d*18:1-18:0 and *d*20:1-18:0 have MWs 1545.8 Da, 1573.9 Da), β -D-GalNAc-(1 \rightarrow 4)-[α -D-Neu5Ac-(2 \rightarrow 3)]- β -D-Gal-(1 \rightarrow 4)-D-Glc-ceramide (GM2, major isoforms *d*18:1-18:0 and *d*20:1-18:0 have MWs 1383.7 Da, 1411.7 Da) and α -D-Neu5Ac-(2 \rightarrow 3)- β -D-Gal-(1 \rightarrow 4)-D-Glc-ceramide (GM3, major isoforms *d*18:1-18:0 and *d*20:1-18:0 have MWs 1180.5 Da, 1208.5 Da) were purchased from Cedarlane Labs (Burlington, Canada); α -D-Neu5Ac-(2 \rightarrow 3)- β -D-Gal-(1 \rightarrow 3)- β -D-GalNAc-(1 \rightarrow 4)-[α -D-Neu5Ac-(2 \rightarrow 3)]- β -D-Gal-(1 \rightarrow 4)-D-Glc-ceramide (GD1a, major isoforms *d*18:1-18:0 and *d*20:1-18:0 have MWs 1836.1 Da, 1864.1 Da), (β -D-Gal-(1 \rightarrow 3)- β -D-GalNAc-(1 \rightarrow 4)-[α -D-Neu5Ac-(2 \rightarrow 8)]- α -D-Neu5Ac-(2 \rightarrow 3)]- β -D-Gal-(1 \rightarrow 4)-D-Glc-ceramide (GD1b, major isoforms *d*18:1-18:0 and *d*20:1-18:0 have MWs 1836.1 Da, 1864.1 Da), α -Neu5Ac-(2-3)- β -D-Galp-(1-3)- β -D-GalNAc-(1-4)-[α -Neu5Ac-(2-8)]- α -

Neu5Ac-(2-3)]- β -D-Galp-(1-4)-D-Glc-ceramide (GT1b, major isoforms *d*18:1-18:0 and *d*20:1-18:0 have MWs 2126.4 Da, 2154.4 Da) were purchased from Sigma-Aldrich Canada (Oakville, Canada), and β -D-GalNAc-(1 \rightarrow 4)-[α -D-Neu5Ac-(2 \rightarrow 8)- α -D-Neu5Ac-(2 \rightarrow 3)]- β -D-Gal-(1 \rightarrow 4)-D-Glc-ceramide (GD2, major isoforms *d*18:1-18:0 and *d*20:1-18:0 have MWs 1674.0 Da, 1702.0 Da) were purchased from MyBioSource Inc. (San Diego, CA). The phospholipid 1-palmitoyl-2-oleoyl-*sn*-glycero-3-phosphocholine (POPC) and porcine brain extract were purchased from Avanti Polar Lipids Inc. (Alabaster, AL). The structures of the gangliosides and POPC are shown in Figure S2, Supporting Information. The procedure for extracting GLs from the A549 cell line culture was described previously.¹⁰

Oligosaccharides

The ganglioside oligosaccharides β -D-Gal-(1 \rightarrow 3)- β -D-GalNAc-(1 \rightarrow 4)-[α -D-Neu5Ac-(2 \rightarrow 3)]- β -D-Gal-(1 \rightarrow 4)-D-Glc (GM1_{os}, MW 998.34 Da); β -D-GalNAc-(1 \rightarrow 4)-[α -D-Neu5Ac-(2 \rightarrow 3)]- β -D-Gal-(1 \rightarrow 4)-D-Glc (GM2_{os}, MW 836.29 Da); α -D-Neu5Ac-(2 \rightarrow 3)- β -D-Gal-(1 \rightarrow 4)-D-Glc (GM3_{os}, MW 633.21 Da); α -D-Neu5Ac-(2 \rightarrow 3)- β -D-Gal-(1 \rightarrow 3)- β -D-GalNAc-(1 \rightarrow 4)-[α -D-Neu5Ac-(2 \rightarrow 3)]- β -D-Gal-(1 \rightarrow 4)-D-Glc (GD1_{aos}, MW 1289.44 Da); β -D-Gal-(1 \rightarrow 3)- β -D-GalNAc-(1 \rightarrow 4)-[α -D-Neu5Ac-(2 \rightarrow 8)- α -D-Neu5Ac-(2 \rightarrow 3)]- β -D-Gal-(1 \rightarrow 4)-D-Glc (GD1_{bos}, MW 1289.44 Da); β -D-GalNAc-(1 \rightarrow 4)-[α -D-Neu5Ac-(2 \rightarrow 8)- α -D-Neu5Ac-(2 \rightarrow 3)]- β -D-Gal-(1 \rightarrow 4)-D-Glc (GD2_{os}, MW 1127.39 Da); α -Neu5Ac-(2-3)- β -D-Galp-(1-3)- β -D-GalNAc-(1-4)-[α -Neu5Ac-(2-8)- α -Neu5Ac-(2-3)]- β -D-Galp-(1-4)-D-Glc (GT1_{bos}, MW 1581.39 Da) were purchased from Elicityl SA (Crolles, France). The structures of the oligosaccharides are shown in Figure S1 (Supporting Information). Stock solutions (1 mM in Milli-Q water (Millipore, MA)) of each of the oligosaccharides were stored at -20 °C until needed.

Picodisc Preparation

Picodiscs containing GLs were prepared using a protocol reported previously¹⁵ and only a brief overview is given here. The phospholipid POPC, dissolved in chloroform, was mixed with either an individual ganglioside, a mixture of gangliosides (GM1, GM2, GM3, GD1a, GD1b, GD2, GT1b) or a GL extract, dissolved in 2:1 chloroform:methanol, in a 4:1 molar ratio. The lipids were dried using nitrogen and kept in a vacuum desiccator overnight at room temperature to form a lipid film. The film was re-dissolved in a buffer of 50 mM sodium acetate and 150 mM NaCl (pH 4.8) followed by sonication and around 10 freeze/thaw cycles to form liposomes. Picodisc formation was initiated by adding SapA protein, at 1:10 molar ratio of SapA-to-total lipid, and incubating at 37 °C for 60 min. A Superdex 75 10/300 size-exclusion column (GE Healthcare Bio-Science, Uppsala, Sweden), equilibrated in 50 mM sodium acetate and 150 mM NaCl (pH 4.8), was used for purification of the PDs. The PD fractions were pooled, concentrated and buffer exchanged into 200 mM ammonium acetate (pH 6.8). The concentration of SapA monomer was determined by measuring the UV absorbance at 280 nm and using an extinction coefficient of 8855 M⁻¹ cm⁻¹. The PDs were concentrated to approximately 100 μM and stored at room temperature until used.

Nanodisc Preparation

Nanodiscs were prepared according to a protocol reported previously.³⁰⁻³² Briefly, DMPC (dissolved in chloroform) was mixed with seven gangliosides GM1, GM2, GM3, GD1a, GD1b, GT1b, GD2 (dissolved in 2:1chloroform:methanol) in the desired ratio (2% for each ganglioside and 86% for DMPC). The lipids were dried under nitrogen and kept in a vacuum desiccator overnight at room temperature to form a lipid film. Lipids were then re-suspended in 20 mM TrisHCl, 0.5 mM EDTA, 100 mM NaCl, 25 mM sodium cholate (pH 7.4) and sonicated for 15 min. MSP1E1 was added at 1:100 molar ratio of MSP1E1-to-total lipid followed by incubation

at room temperature for 15 min. An equal volume of Bio-Beads (Bio-Rad Laboratories Ltd., Mississauga, Canada) was added to initiate ND formation and the solution was incubated at room temperature for 3 h to remove all detergent. Finally, a Superdex 200 10/300 size exclusion column (GE Healthcare Bio-Sciences, Uppsala, Sweden), which was equilibrated in 200 mM ammonium acetate (pH 6.8), was used for purification of the NDs. Nanodiscs were concentrated to approximately 60 μ M and stored at -80 °C until needed.

Mass Spectrometry

The ESI-MS and CaR-ESI-MS measurements were carried out using a Synapt G2S quadrupole-ion mobility separation-time-of-flight (Q-IMS-TOF) mass spectrometer (Waters, Manchester, UK) equipped with a nanoESI source. The CaR-ESI-MS assay was implemented in negative ion mode, whereas the direct ESI-MS assay was performed in positive ion mode. Borosilicate capillaries (1.0 mm o.d., 0.68 mm i.d.) were pulled using a P-1000 micropipette puller (Sutter Instruments, Novato, CA). A platinum wire was inserted into the nanoESI tip and a capillary voltage of -0.9 kV (negative ion mode) or 1.0 kV (positive ion mode) was applied to carry out ESI. The source temperature was 60 °C for both two modes. A cone voltage of 30 V was used and the Trap and Transfer collision energies were set to 5 and 2 V, respectively, for ESI-MS analysis. All data were processed using MassLynx software (version 4.1) and Driftscope v.2.5 (Waters, Manchester, UK).

CaR-ESI-MS assay

To implement the CaR-ESI-MS assay, the quadrupole mass filter was set (to HM 15 and LM 4) to pass ions with a range of mass-to-charge ratios (m/z) (actual window, which was determined based on changes in background signal, ranges from 100 to 200 m/z) that encompasses the ions corresponding to the free and GL-bound protein of interest at a given charge state. Collision-

induced dissociation (CID) was performed in the Trap region using collision energies of 50 to 100 V. The released ganglioside anions were identified based on their measured MWs. Where MW alone was insufficient for positive GL identification, CID of the corresponding ions, produced directly from solution, was carried out in the Transfer region using a collision energy of 75 V. In cases where the free and GL-bound protein ions and those corresponding to the PDs overlapped in the mass spectrum, ion mobility separation (IMS) was used to separate the protein (and protein-GL complexes) from the PD ions; release of the GL ions was achieved by CID performed in the Transfer region using collision energies of between 50 V and 75 V. For IMS measurements, a wave height of 40 V and a wave velocity of between 650 m s⁻¹ and 850 m s⁻¹ were applied and helium and nitrogen (IMS gas) gas flow rates of 50 mL min⁻¹ and 60 mL min⁻¹, respectively, were used.

Direct ESI-MS assay

The direct ESI-MS assay was used to quantify the binding of seven ganglioside oligosaccharides (GM1_{os}, GM2_{os}, GM3_{os}, GD1a_{os}, GD1b_{os}, GD2_{os}, GT1b_{os}) to CTB₅.³³ Binding measurements were carried out in triplicate using a fixed protein concentration and five different oligosaccharide concentrations. The reference protein (P_{ref}) method was used to correct the mass spectra for the occurrence of non-specific carbohydrate-protein binding during ESI.³⁴ The scFv, which does not bind to the oligosaccharides tested, served as P_{ref}. Although CTB₅ has five carbohydrate binding sites, only a single site was found to be occupied under the solution conditions used. Consequently, a 1:1 protein (P)-ligand (L) binding model (eq 1) was used to analyze the ESI-MS data. The apparent association constant (K_a) was calculated using eq 2:



$$K_a = \frac{R}{[L]_0 - \frac{R}{1+R}[P]_0} \quad (2)$$

where $[P]_0$ and $[L]_0$ are the initial concentrations of P and L, respectively. The abundance ratio (R) of the ligand-bound protein (PL) to free protein (P) ions measured by ESI-MS (after correction for non-specific binding)³⁴ is taken to be equal to the equilibrium concentration ratio in solution, eq 3:

$$R = \frac{\sum Ab(PL)}{\sum Ab(P)} = \frac{[PL]}{[P]} \quad (3)$$

Results and discussion

The main objective of this study was to establish the feasibility of using PDs to solubilize mixtures of GLs and screen them against water-soluble target proteins using the CaR-ESI-MS assay. With this goal in mind, four libraries of GL-containing PDs were prepared. Two of the libraries (*Library 1* and *Library 2*) contained seven gangliosides (GM1, GM2, GM3, GD1a, GD1b, GD2 and GT1b) - *Library 1* consisted of an equimolar mixture of seven different PDs, each prepared with a single ganglioside, while *Library 2* consisted of PDs prepared from an equimolar mixture of the seven gangliosides. To confirm that all seven gangliosides were incorporated into the PDs, the two libraries were analyzed by ESI-MS and the PD ions subjected to CID. Shown in Figure S3 (Supporting Information) are the ESI mass spectra for aqueous ammonium acetate solutions (200 mM, pH 6.8) of each library (total ganglioside concentration 140 μ M). In both cases, a broad unresolved peak centered at approximately m/z 4800 was observed. This feature is attributed to the intact PD ions.¹³ The quadrupole was set to pass ions with $m/z > 4000$, which were then subjected to CID in the Trap region. At collision energies of 30 V to 100 V, signal corresponding to all seven deprotonated ganglioside ions was detected. At

energies ≥ 50 V, secondary fragmentation of the ganglioside ions resulted in the appearance of deprotonated Neu5Ac (m/z 290) and deprotonated α -D-Neu5Ac-(2 \rightarrow 8)- α -D-Neu5Ac (m/z 581) (Figure S4, Supporting Information). These results confirm that all seven gangliosides were successfully incorporated into the PDs. *Library 3* and *Library 4* consisted of a mixture of GLs extracted from porcine brain and a mixture of GLs extracted from cultured human epithelial A549 cell line, respectively. All four libraries were screened against CTB₅, only *Library 2* was screened against TcdA-A2.

Previously, the GLs found in *Library 2*, *Library 3* and *Library 4* were screened against CTB₅ using the CaR-ESI-MS assay implemented with NDs.^{1,2} In order to have a complete set of comparative data, the CaR-ESI-MS assay, implemented with NDs, was also used in the present study to screen a mixture of seven gangliosides against TcdA-A2. The NDs used for these measurements consisted of equimolar amounts (2% of each ganglioside) of GM1, GM2, GM3, GD1a, GD1b, GD2, GT1b. These NDs are referred to as the 7G NDs. Shown in Figure S5a (Supporting Information) is a representative ESI mass spectrum acquired for an aqueous ammonium acetate (200 mM, pH 6.8) solution of 7G ND (6 μ M). The broad peak centered at m/z ~11000 is attributed to intact ND. CID was carried out on all ions with m/z >5600 in the Trap region with a collision energy of 150 V and resulted in the appearance of all seven deprotonated ganglioside ions, confirming their incorporation into the NDs (Figure S5b, Supporting Information).

a. Screening Ganglioside-Containing PDs against CTB₅

The CaR-ESI-MS assay was used to screen *Library 1* and *Library 2* against CTB₅. Shown in Figure 1a is a representative ESI mass spectrum acquired in negative ion mode for an aqueous ammonium acetate solution (200 mM, pH 6.8) of CTB₅ (3 μ M) and *Library 1* (6 μ M, each

ganglioside). Signal corresponding to the -12 to -15 charge states of the deprotonated ions of CTB₅ and CTB₅ bound to one or two ganglioside molecules (i.e., (CTB₅ + L)ⁿ⁻ and (CTB₅ + 2L)ⁿ⁻), as well as PD ions, is evident. Peak assignments were made using the measured and theoretical m/z values and assuming that L corresponds predominantly to GM1. Because of spectral overlap of ions corresponding to the free and GL-bound CTB₅ and those of the PDs, IMS was used to separate the CTB₅ ions from PD ions (Figures 1b and 1c). To identify the gangliosides bound to CTB₅, CID (in the Transfer region) was performed simultaneously on the (CTB₅ + L)ⁿ⁻ and (CTB₅ + 2L)ⁿ⁻ ions, at charge states -12 to -15, post-IMS. Using a collision energy of 75 V, CID resulted predominantly in the release of singly deprotonated GM1 ions, with singly deprotonated GM2, GM3, GD1a and/or GD1b ions and doubly deprotonated GT1b detected, but at lower abundance (Figure 1d). Because GD1a and GD1b are structural isomers, they cannot be distinguished based on mass. Moreover, because CID was performed post-IMS, it was not possible to confirm the identity of the two gangliosides based on differences in IMS arrival times. Therefore, the CaR-ESI-MS measurements were repeated using PDs containing only GD1a or GD1b. These results confirmed that both GD1a and GD1b bind to CTB₅ under these solution conditions (Figure S6, Supporting Information). Based on the results of this analysis, it is concluded that GM1, GM2, GM3, GT1b, GD1a and GD1b bind to CTB₅, with no evidence of GD2 binding. Moreover, the relative abundances of the released ligands are consistent with GM1 having a higher affinity than the other gangliosides. These findings are consistent with binding data measured for CTB₅ and the oligosaccharides of these seven gangliosides, *vide infra*.

Measurements were also carried out on an aqueous ammonium acetate solution (200 mM, pH 6.8) of CTB₅ (3 μM) and *Library 2* (42 μM, 6 μM of each ganglioside). The ESI mass

spectrum acquired post-IMS, Figure 2a, is qualitatively similar to that measured for solutions containing *Library 1*. At these concentrations, signals corresponding to the -12 to -15 charge states of free CTB₅ and CTB₅ bound to one or two ganglioside molecules (i.e., (CTB₅ + L)ⁿ⁻ and (CTB₅ + 2L)ⁿ⁻ were detected. CID of all the (CTB₅ + L)ⁿ⁻ and (CTB₅ + 2L)ⁿ⁻ ions in the Transfer region, using a collision energy of 75 V, led primarily in the appearance of singly deprotonated GM1 ions, with signal corresponding to GM2, GM3, GT1b ions also evident (Figure 2b). Signal corresponding to deprotonated ions of GD1a and/or GD1b was also detected. Based on the results described above, it is reasonable to assume that the signal corresponds to the presence of both isomers. The CaR-ESI-MS measurements were also performed using a higher concentration of *Library 2*. Shown in Figure 2c is a representative ESI mass spectrum acquired for an aqueous ammonium acetate solution (200 mM, pH 6.8) of CTB₅ (3 μM) and *Library 2* (63 μM, 9 μM of each ganglioside). Notably, at the higher library concentration, CTB₅ was found to bind between one and five gangliosides. Post-IMS CID of the (CTB₅ + iL)ⁿ⁻ ions, where *i* = 1 to 5, at charge states -12 to -15 resulted primarily in the appearance of singly deprotonated GM1 ions, with GM2, GM3, GT1b, GD1a/GD1b ions also detected (Figure 2d). These results are consistent with those obtained at the lower *Library 2* concentration (Figure 2a).

To exclude the possibility of false positives resulting from the formation non-specific protein-ganglioside interactions during the ESI process, the CaR-ESI-MS assay was also used to screen *Library 2* against Stx1-B₅, which served as a negative control. Stx1, like CT, belongs to the family of AB₅ bacterial toxins. However, to the best of our knowledge, Stx1-B₅ (and Stx1) has no affinity for gangliosides. Shown in Figure S7 (Supporting Information) is a representative ESI mass spectrum acquired for an aqueous ammonium acetate solution (200 mM, pH 6.8) of Stx1-B₅ (5 μM) and *Library 2* (56 μM, 8 μM of each ganglioside). Notably, no signal

corresponding to Stx1-B₅ bound to any of the gangliosides was detected; instead, the only protein ion signal corresponded to free Stx1-B₅. The absence of ganglioside binding was further shown by CID, performed in the Trap region on the Stx1-B₅ ions, which failed to produce any signal corresponding to ganglioside ions. These results suggest that nonspecific binding of proteins to GLs contained within the PDs during the ESI process is negligible.

Based on the results described above, it is concluded that CTB₅ binds to GM1, GM2, GM3, GT1b, GD1a and GD1b, but not GD2. Interestingly, screening this same mixture of gangliosides against CTB₅ using the CaR-ESI-MS assay implemented with NDs revealed binding to GM1, GM2, GM3, GD1a and GD1b, but not to GT1b or GD2.¹¹ The relative affinities of six of these gangliosides for CTB₅ were previously investigated using SPR spectroscopy and found to be in the order: GM1 > GM2 > GD1a > GM3 > GT1b > GD1b;¹⁸ no binding to GD2 has been reported.³⁵⁻³⁶ Consequently, it would seem that the CaR-ESI-MS results obtained using the PDs are in better agreement with the reported CTB₅ binding data than those measured using NDs. To further support this conclusion, affinity measurements were carried out using the direct ESI-MS assay on CTB₅ and the oligosaccharides of the seven gangliosides found in *Library 1* and *Library 2*. To the best of our knowledge, quantitative affinity data for CTB₅ binding to ganglioside oligosaccharides are only available for the GM1 pentasaccharide (GM1_{os}).¹⁹ Because the affinities of the other ganglioside oligosaccharides for CTB₅ are low, the ESI-MS binding measurements were carried out using a titration format, wherein the concentration of CTB₅ was fixed at 6 μM and the concentration of oligosaccharide was varied from 0 to 100 μM. A reference protein (P_{ref}) was added in all experiments to correct nonspecific protein-carbohydrate interactions during the ESI process.³⁴ Representative ESI mass spectra acquired for an aqueous ammonium acetate (200 mM, pH 6.8) solution of CTB₅ (6 μM), P_{ref} (2 μM), and each of the

oligosaccharides (60 μM) are shown in Figure S8 (Supporting Information); the corresponding titration plots are shown in Figure S9 (Supporting Information). From the ESI-MS data, apparent K_a values were calculated for each oligosaccharide (Table 1). Inspection of Table 1 reveals that GM2_{os} , GM3_{os} , GD1a_{os} , GD1b_{os} and GT1b_{os} exhibit low, but measurable, affinities, in the 500 M^{-1} range, while GD2 does not bind. Notably, these results are in agreement with the results obtained from the CaR-ESI-MS assay implemented with the PDs. At present it is not known why the GT1b interaction with CTB_5 was not detected when using NDs; however, it should be noted that the CaR-ESI-MS assay implemented with NDs has produced false negatives for other low affinity protein-GL interactions.¹¹

b. Screening PDs and NDs containing known GLs against TcdA-A2

Taken together, the results obtained for CTB_5 and the PD-based ganglioside libraries show that the CaR-ESI-MS assay combined with PDs can be used to screen mixtures of GLs against proteins and simultaneously detect both low and high affinity protein-GL interactions. To demonstrate the general utility of the assay, it was also applied to screen *Library 2* against TcdA-A2. Shown in Figure 3a is a representative ESI mass spectrum acquired for an aqueous ammonium acetate (200 mM, pH 6.8) solution of TcdA-A2 (6 μM) and *Library 2* (120 μM , 17 μM each ganglioside). Signals corresponding to the -9 to -12 charge states of free and ganglioside-bound TcdA-A2 (i.e. $(\text{TcdA-A2} + \text{L})^{n-}$) ions were detected (along with a broad feature attributed to the PD ions, *vide supra*). CID, carried out in Trap, of the $(\text{TcdA-A2} + \text{L})^{10-}$ ions resulted in the appearance of singly deprotonated GM3 , GM2 , GM1 , GD1a and/or GD1b ions and doubly deprotonated GT1b , GD1a and/or GD1b ions, as well as TcdA-A2 ions (Figure 3c). These results suggest that TcdA-A2 exhibits broad specificity for gangliosides and binds GM1 , GM2 , GM3 , GT1b , GD1a and/or GD1b , although, presumably, with low affinity. CaR-

ESI-MS measurements performed using PDs containing only GD1a or GD1b revealed that only GD1a bind to TcdA-A2 under these solution conditions (Figure S10, Supporting Information). Like CTB₅, TcdA-A2 was found not to bind GD2. These results are in qualitative agreement with affinity measurements, which reveal that the oligosaccharides of GM1, GM2, GM3, GT1b and GD1a, but not GD2, bind to TcdA-A2, with association constants in the 1000 M⁻¹ range.²⁷

To further compare the performance of PDs to NDs for GL screening, the CaR-ESI-MS assay was implemented using NDs to screen the same seven gangliosides against TcdA-A2. Shown in Figure 3d is a representative ESI mass spectrum acquired in negative ion mode for an aqueous ammonium acetate (200 mM, pH 6.8) solution of TcdA-A2 (6 μM) and 7G NDs (20 μM, which contain 2% of each of the seven gangliosides). A broad peak centered at $m/z \sim 10000$, which is attributed to intact ND ions, as well as signals corresponding to TcdA-A2ⁿ⁻ and (TcdA-A2 + L)ⁿ⁻ ions, at charge states -8 to -11, can be identified in the mass spectrum. Also present are ion signals corresponding to TcdA-A2 bound to DMPC, which was used to prepare the NDs. To ascertain the identity of the GL ligands, the quadrupole mass filter was set to pass all possible (TcdA-A2 + L)¹⁰⁻ ions; these were then subjected to CID in the Trap. Analysis of the CID results revealed TcdA-A2 binding to GM1, GM2, GM3 (Figure 3f). However, the assay failed to detect binding to GT1b or GD1a. These results, taken together with the false negatives reported above and elsewhere,¹³ suggest that PDs are to be preferred over NDs for detection of low affinity protein-GL interactions by ESI-MS.

c. Screening PDs prepared from glycolipid extracts against CTB₅

The results described above establish the reliability of the CaR-ESI-MS assay, implemented with PDs of known composition, to screen libraries of GLs against target proteins *in vitro*. To further illustrate the utility of the assay, measurements were also carried out using PDs prepared using

GLs extracted from porcine brain (*Library 3*). This extract is known to consist primarily of ten different gangliosides and seventeen sulphatides.³⁷ ESI mass spectra acquired post-IMS for an aqueous ammonium acetate (200 mM, pH 6.8) solution of CTB₅ (5 μM) and *Library 3* (at an estimated (based on the mass concentration of extract and an estimated average molecular weight for the lipids) concentration of 78 μM) revealed signal corresponding to free CTB₅ⁿ⁻ and (CTB₅ + L)ⁿ⁻ ions (Figure 4a). CID performed simultaneously on (CTB₅ + L)ⁿ⁻ ions at charge states -12 to -15 in the Transfer region resulted in the appearance of deprotonated GM1 ions (isoform *d18:1-18:0*, *m/z* 1545.09 and isoform *d20:1-18:0*, *m/z* 1573.12), as well as singly charged ions at *m/z* 1690.83 (L_{a1}) and *m/z* 1718.86 (L_{b1}), along with CTB monomer (Figure 4b). The identities of the L_{a1} and L_{b1} were established by subjecting these ions (produced directly from a methanol solution of the extracted lipids) to CID. Based on the fragment ions produced, (B₀-H₂)⁻, Y₀⁻, Y₁⁻, Y₂-Neu5Ac⁻ and Y₄⁻ (Figure S11, Supporting Information) it was concluded that L_{a1} and L_{b1} are two isoforms (*d18:1-18:0* and *d20:1-18:0*) of fucosyl-GM1 (α-L-Fuc-(1→2)-β-D-Gal-(1→3)-β-D-GalNAc-(1→4)-[α-D-Neu5Ac-(2→3)]-β-D-Gal-(1→4)-D-Glc-ceramide). It has been previously reported that CTB₅ binds with fucosyl-GM1 oligosaccharide with high affinity.³⁸

Measurements were also carried out on PDs prepared from GLs extracted from the A549 carcinomic human alveolar basal epithelial cell line (*Library 4*). CaR-ESI-MS performed on an aqueous ammonium acetate (200 mM, pH 6.8) solution of CTB₅ (5 μM) and *Library 4* yielded signal corresponding to free CTB₅ and CTB₅ bound to one GL (Figure 4c). CID performed in the Transfer region on (CTB₅ + L)ⁿ⁻ ions, at charge states -12 to -15, resulted in the appearance of CTB monomer and singly deprotonated ions with *m/z* 1517.02 (L_{a2}), *m/z* 1545.07 (L_{b2}), *m/z* 1573.09 (L_{c2}) and *m/z* 1629.15 (L_{d2}). CID of the L_{a2}⁻, L_{b2}⁻, L_{c2}⁻ and L_{d2}⁻ ions, produced by ESI performed on a methanol solution of A549 cell line extract, produced (B₀-H₂)⁻, Y₀⁻, Y₁⁻, and Y₂-

Neu5Ac⁻ fragment ions (Figure S12, Supporting Information). Based on the CID results, the four ions were identified as isoforms of GM1 (*d*16:1-18:0 (or *d*18:1-16:0), *d*18:1-18:0, *d*20:1-18:0, *d*20:1-22:0 (or *d*18:1-24:0), Figure 4b). Notably, these results are consistent with those obtained previously using the CaR-ESI-MS assay implemented with NDs.¹¹

Conclusions

The results of the present study demonstrate the utility of the CaR-ESI-MS assay, implemented with PDs, for screening libraries of GLs against water-soluble proteins *in vitro* to identify specific interactions. Application of the assay to screen a small library of gangliosides against CTB₅ and TcdA-A2 demonstrated that both high and low affinity interactions can be detected simultaneously. Notably, comparison of the screening results with affinity data for the corresponding ganglioside oligosaccharides indicates that the assay produced no false positives or false negatives. Moreover, implementation of the assay using PDs prepared from GLs extracted from tissue or cell culture successfully identified high affinity ganglioside ligands present in both GL mixtures. Finally, a comparison of the present results with data obtained with the CaR-ESI-MS assay implemented using NDs revealed that the PDs exhibit similar or superior performance to NDs for protein-GL binding measurement and that PDs are to be preferred over NDs for detection of low affinity protein-GL interactions.

ASSOCIATED CONTENT

Supporting Information

Mass spectra and structures. This information is available free of charge via the Internet at <http://pubs.acs.org/>.

Author Information

Corresponding Author

john.klassen@ualberta.ca

Notes

The authors declare no competing financial interests.

Acknowledgement

The authors are grateful for financial support provided by the National Sciences and Research Council of Canada and the Alberta Glycomics Centre (J.S.K., C.W.C. and K.K.S.N.) and the Canadian Institutes of Health Research (G.G.P.). We also acknowledge G. Armstrong (University of Calgary) for generously providing protein used in this study.

References

1. Hakomori, S. *Curr. Opin. Hematol.* **2003**, *10*, 16-24.
2. Varki, A.; Cummings, R. D.; Esko, J. D.; Freeze, H. H.; Stanley, P.; Bertozzi, C. R.; Hart, G. W.; Etzler, M. E. *Essentials of Glycobiology*, 2nd ed.; Cold Spring Harbor Laboratory Press: Cold Spring Harbor, NY, 2009.
3. Malhotra, R. *Biochem Anal Biochem* **2012**, *1*, 108.
4. Schulze, H.; Sandhoff, K. *Biochim. Biophys. Acta* **2014**, *1841*, 799-810.
5. Lopez, H. H. H.; Schnaar, R. L. *Methods Enzymol.* **2006**, *417*, 205–220.
6. Lipid-Protein Interactions. In *Methods and Protocols*; Kleinschmidt, J. H., Ed.; Springer: New York, 2014; Vol. 974.
7. Evans, S. V.; Roger MacKenzie. C. *J. Mol. Recognit.* **1999**, *12*, 155-68.
8. Lingwood, C. A.; Manis, A.; Mahfoud, R.; Khan, F.; Binnington, B.; Mylvaganam, M. *Chem. Phys. Lipids.* **2010**, *163*, 27-35.
9. Czogalla, A.; Grzybek, M.; Jones, W.; Coskun, U. *Biochim. Biophys. Acta* **2014**, *1841*, 1049-1859.
10. Zhang, Y.; Liu, L.; Daneshfar, R.; Kitova, E. N.; Li, C.; Jia, F.; Cairo, C.W.; Klassen, J. S. *Anal. Chem.* **2012**, *84*, 7618-7621.
11. Leney, A.; Fan, X.; Kitova, E.N.; Klassen, J. S. *Anal. Chem.* **2014**, *86*, 5271-5277.
12. Han, L.; Kitova, E. N.; Li, J.; Nikjah, S.; Lin, H.; Pluvinaige, B.; Boraston, A. B.; Klassen, J. S. *Anal. Chem.* **2015**, *87*, 4888-4896.
13. Leney, A. C.; Darestani, R. R.; Li, J.; Nikjah, S.; Kitova, E. N.; Zou, C.; Cairo, C. W.; Xiong, Leney, A.; Fan, X.; Kitova, E. N.; Klassen, J. S. *Anal. Chem.* **2015**, *87*, 4402-4408.
14. Bayburt, T. H.; Grinkova, Y. V.; Sligar, S. G. *Nano Lett.* **2002**, *2*, 853–856.

15. Popovic, K.; Holyoake, J.; Pomès, R.; Privé, G.G. *Prot. Natl. Acad. Sci.* **2012**, *109*, 2908-2912.
16. Merritt, E. A.; Sarfaty, S.; Van Den Akker, F.; L'Hoir, C.; Martial, J. A.; Hol, W. G. J. *Protein Sci.* **1994**, *3*, 166–175.
17. Holmgren, J.; Lönnroth, I.; Svennerholm, L. *Infect. Immun.* **1973**, *8*, 208-214.
18. Kuziemko, G. M.; Stroh, M.; Stevens, R. C. *Biochemistry* **1996**, *35*, 6375-6384.
19. Lin, H.; Kitova, E. N.; Klassen, J. S. *J. Am. Soc. Mass Spectrom.* **2014**, *25*, 104–110.
20. Just, I.; Gerhard, R. Large clostridial cytotoxins. In *Reviews of Physiology, Biochemistry and Pharmacology*, Springer Berlin Heidelberg: **2005**, *152*, 23-47.
21. Dallas, S. D.; Rolfe, R. D. *J. Med. Microbiol.* **1998**, *47*, 879-888.
22. Krivan, H. C.; Clark, G. F.; Smith, D. F.; Wilkins, T. D. *Infect. Immun.* **1986**, *53*, 573-581.
23. Smith, J. A.; Cooke, D. L.; Hyde, S.; Borriello, S. P.; Long, R. G. *J. Med. Microbiol.* **1997**, *46*, 953-958.
24. Tucker, K. D.; Wilkins, T. D. *Infect. Immun.* **1991**, *59*, 73-78.
25. Karlsson, K. A. *Curr. Opin. Struct. Biol.* **1995**, *5*, 622-635.
26. Teneberg, S.; Lönnroth, I.; Lopez, J. F. T.; Galili, U.; Halvarsson, M. O.; Angstrom, J.; Karlsson, K. A. *Glycobiology* **1996**, *6*, 599-609.
27. Fan, X.; Kitova, E. N.; Eugenio, L.; Ng, K. K. S.; Klassen, J. S. *manuscript in preparation*
28. Greco, A.; Ho, J. G. S.; Lin, S. J.; Palcic, M. M.; Rupnik, M.; Ng, K. K. S. *Nat. Struct. Mol. Biol.* **2006**, *13*, 460-461.
29. Zdanov, A.; Li Y.; Bundle, D. R.; Deng, S. J.; Mackenzie, C. R.; Narang, S. A.; Young, N. M.; Cygler, M. *Proc. Natl. Acad. Sci. USA.* **1994**, *91*, 6423-6427.

30. Bayburt, T. H.; Grinkova, Y. V.; Sligar, S. G. *Nano Lett.* **2002**, *2*, 853–856.
31. Borch, J.; Torta, F.; Sligar, S. G.; Roepstorff, P. *Anal. Chem.* **2008**, *80*, 6245–6252.
32. Bayburt, T. H.; Sligar, S. G. *FEBS Lett.* **2010**, *584*, 1721–1727.
33. Kitova, E. N.; El-Hawiet, A.; Schnier, P. D.; Klassen, J. S. *J. Am. Soc. Mass Spectrom.* **2012**, *23*, 431-441.
34. Sun, J.; Kitova, E. N.; Wang, W.; Klassen, J. S. *Anal. Chem.* **2006**, *78*, 3010–3018.
35. Teneberg, S.; Hirst, T. R.; Angström, J.; Karlsson, K. A.; *Glycoconj. J.* **1994**, *11*, 533-540.
36. MacKenzie, C. R.; Hiramata, T.; Lee, K. K.; Altman, E.; Young, N. M. *J. Biol. Chem.* **1997**, *272*, 5533-5538.
37. Ikeda, K.; Shimizu, T.; Taguchi, R. *J. Lipid Res.* **2008**, *49*, 2678– 2689.
38. Masserini, M.; Freire, E.; Palestini, P.; Calappi, E.; Tettamanti, G. *Biochemistry.* **1992**, *31*, 2422-2426.

Table 1. Apparent association constants ($K_{a,app}$) for CTB₅ binding to the oligosaccharides (L) of seven gangliosides measured in an aqueous ammonium acetate solution (200 mM) at pH 6.8 and 25 °C using the direct ESI-MS assay.^a

L	$K_{a,app}$ (M ⁻¹)
GM1 _{os}	$(16.0 \pm 1.2) \times 10^6$ ^b
GM2 _{os}	580 ± 130
GM3 _{os}	370 ± 40
GD1a _{os}	480 ± 150
GD1b _{os}	350 ± 50
GD2 _{os}	NB ^c
GT1b _{os}	240 ± 60

a. The reported errors are one standard deviation. b. Apparent association constants for the binding of a single GM1_{os} to CTB₅. c. NB \equiv No binding detected.

Figure captions

Figure 1. ESI mass spectra acquired in negative ion mode for a 200 mM aqueous ammonium acetate solution (pH 6.8, 22 °C) containing CTB₅ (3 μM) and *Library 1* (6 μM) (a) before and (b) after separation of the CTB₅ ions from the PD ions using IMS. (c) Corresponding IMS heat map (plot of ion m/z, ion intensity and IMS arrival times). (d) CID mass spectrum acquired in the Transfer region (post IMS) for the CTB₅ ions, produced from the solution described in (a) and (b), performed in the Transfer region using a collision energy of 75 V.

Figure 2. ESI mass spectra acquired in negative ion mode for a 200 mM aqueous ammonium acetate solution (pH 6.8, 22 °C) containing CTB₅ (3 μM) and *Library 2* at (a) 42 μM or (c) 63 μM; PD ions were excluded from the mass spectrum using IMS. (b) and (d) CID mass spectra acquired in the Transfer region (post IMS separation) for the CTB₅ ions, produced from the solution described in (a) and (c), respectively, performed in the Transfer region using a collision energy of 75 V.

Figure 3. (a) and (b) ESI mass spectrum acquired in negative ion mode for a 200 mM aqueous ammonium acetate solution (pH 6.8, 22 °C) containing TcdA-A2 (6 μM) and *Library 2* (120 μM, 17 μM each ganglioside). (c) CID mass spectrum acquired in the Trap region for the (TcdA-A2 + L)¹⁰⁻ ions using a collision energy of 50 V. (d) and (e) ESI mass spectrum acquired in negative ion mode for a 200 mM aqueous ammonium acetate solution (pH 6.8, 22 °C) containing TcdA-A2 (6 μM) and 7G ND (20 μM, 2% for each ganglioside). (f) CID mass spectrum

acquired in the Trap region for the (TcdA-A2 + L)¹⁰⁻ ions using a collision energy of 50 V.

Figure 4. ESI mass spectra acquired in negative ion mode for a 200 mM aqueous ammonium acetate solution (pH 6.8, 22 °C) containing CTB₅ (5 μM) and (a) *Library 3* (78 μM) or (c) *Library 4*, after separation of the CTB₅ ions from the PD ions using IMS. (b) and (d) CID mass spectra acquired in the Transfer region (post IMS separation) for the CTB₅ ions, produced from the solution described in (a) and (c), respectively, performed in the Transfer region using a collision energy of 75 V.

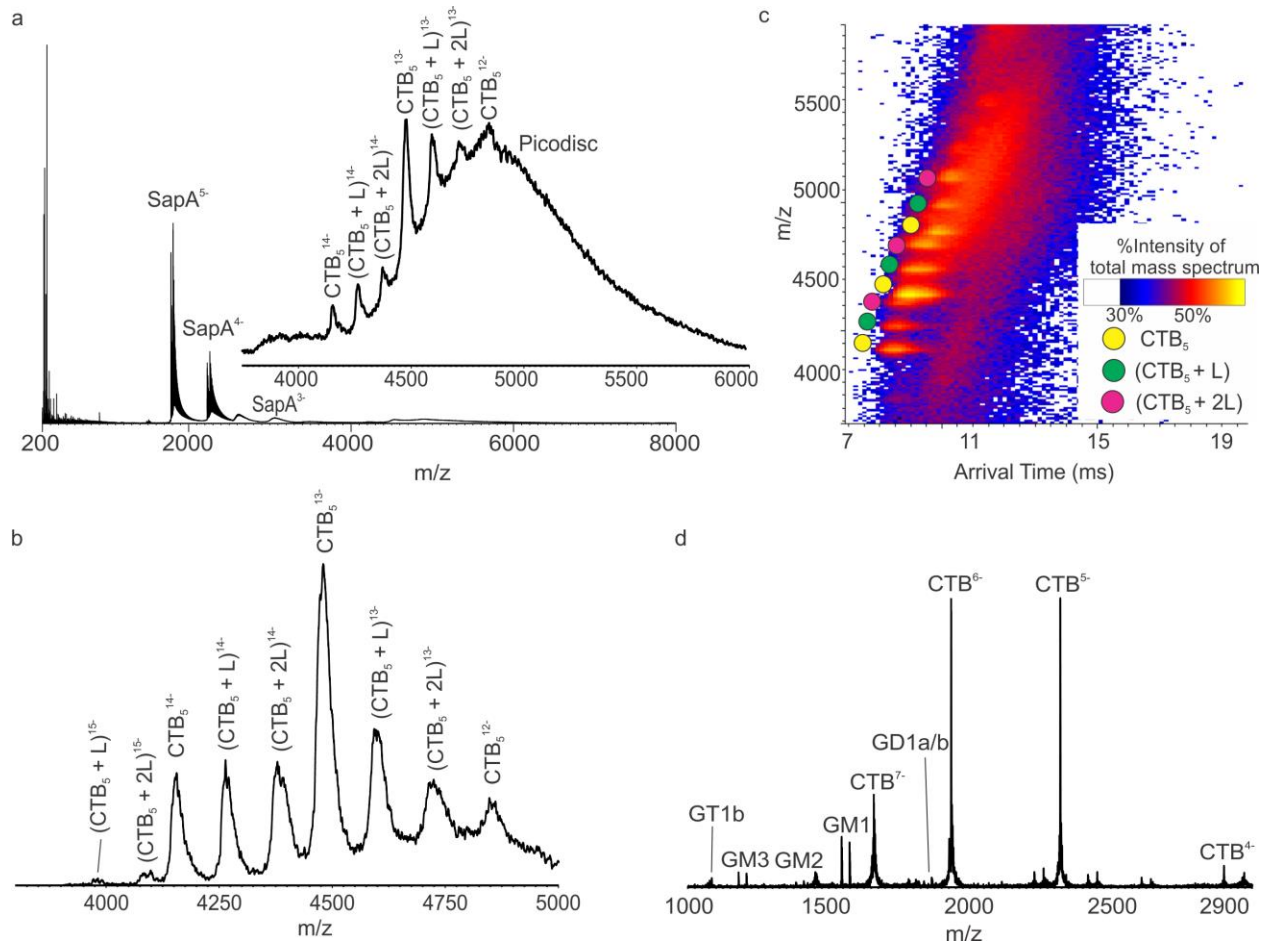


Figure 1

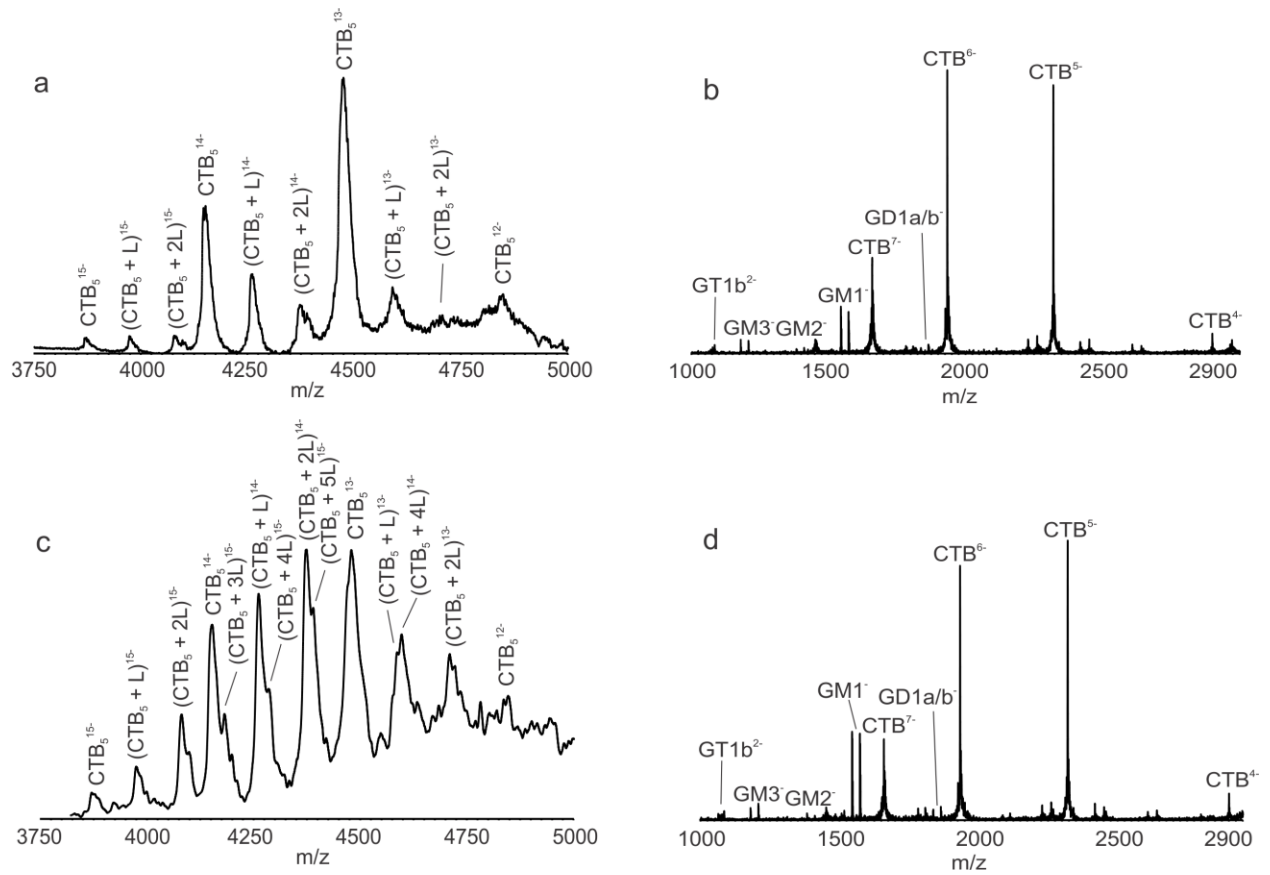


Figure 2

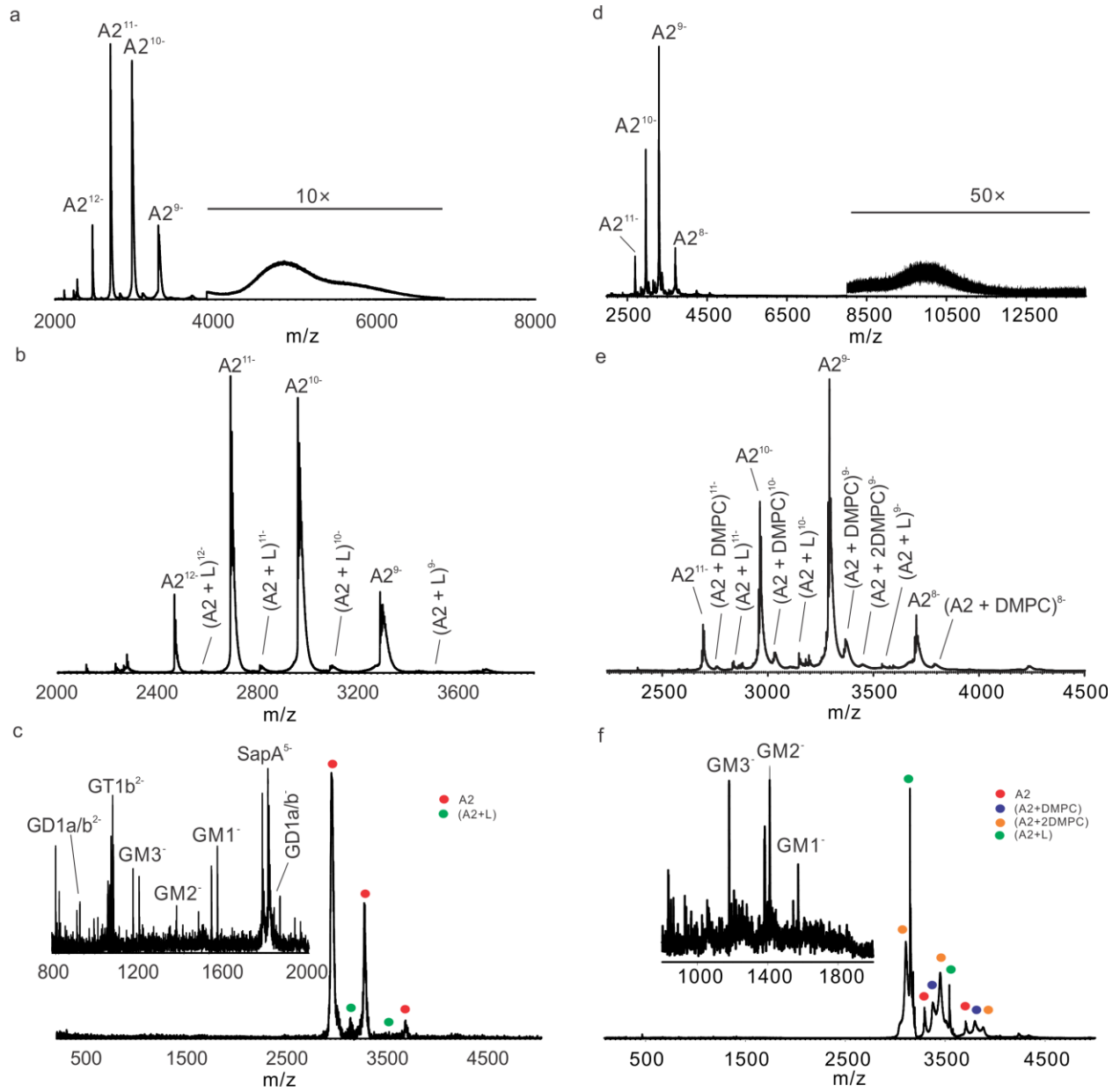


Figure 3

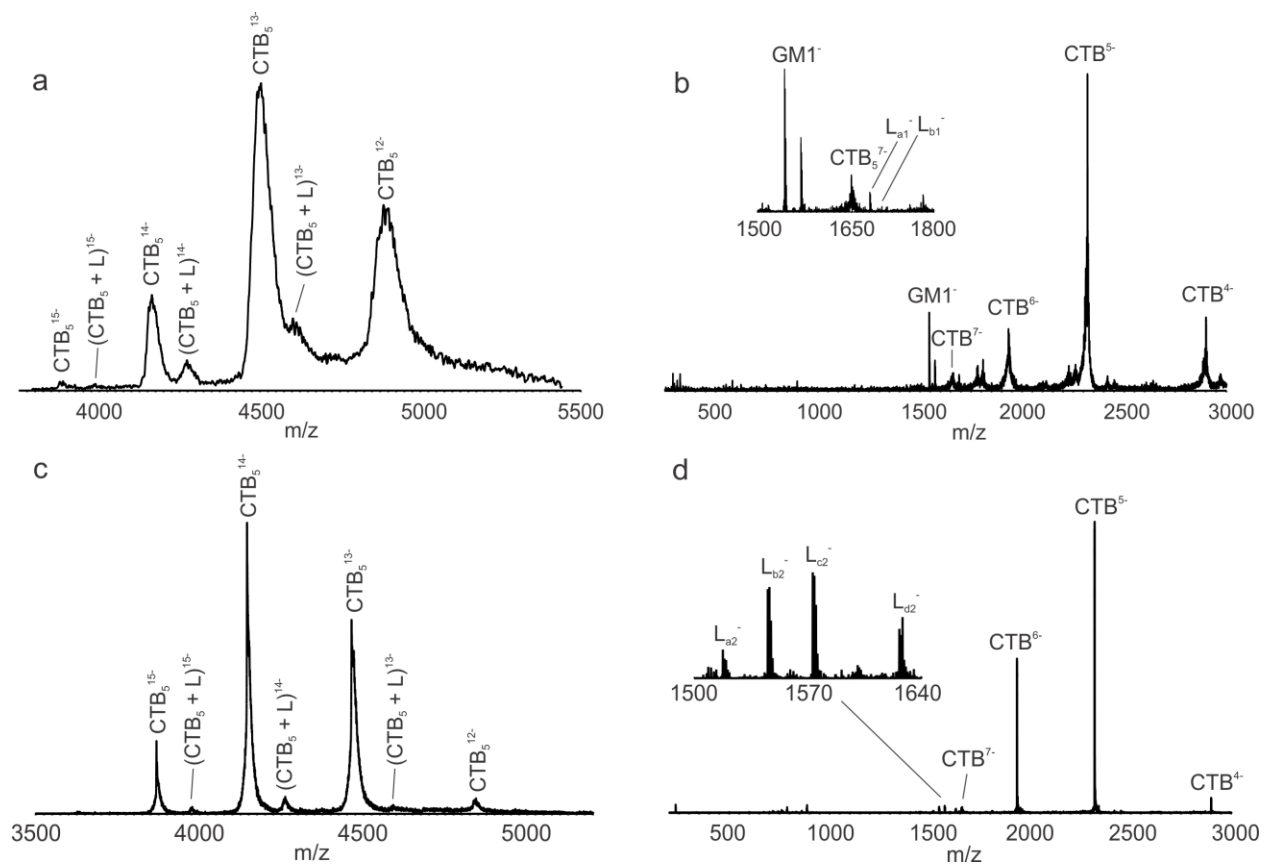
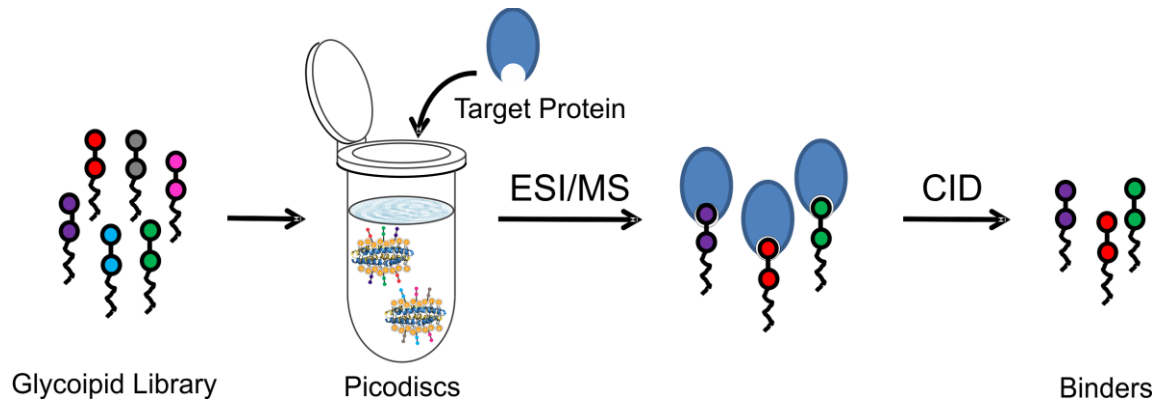


Figure 4

TOC graphic



SUPPORTING INFORMATION FOR:

**Screening Glycolipids Against Proteins in vitro using Picodiscs and
Catch-and-Release Electrospray Ionization Mass Spectrometry**

Jun Li,^{1,2} Xuxin Fan,^{1,2} Elena N. Kitova,^{1,2} Chunxia Zou,^{1,2} Christopher W. Cairo,^{1,2} Luiz
Eugenio,^{1,3} Kenneth K. S. Ng,^{1,3} Zi Jian Xiong,⁴ Gilbert G. Privé,^{4,5} John S. Klassen^{1,2*}

¹*Alberta Glycomics Centre*

²*Department of Chemistry, University of Alberta, Edmonton, Alberta, Canada T6G 2G2*

³*Department of Biological Sciences, University of Calgary, Calgary, Alberta, Canada T2N 1N4*

⁴*Department of Biochemistry, University of Toronto, Toronto, Ontario, Canada M5S 1A8*

⁵*Princess Margaret Cancer Centre, University Health Network, Toronto, Ontario, Canada*

M5G 1L7

*Email: john.klassen@ualberta.ca

Table of Contents

Table S1. Lipid composition of <i>Library 1</i> , <i>Library 2</i> , <i>Library 3</i> and <i>Library 4</i>	S-4
Figure S1. Structures of the ganglioside oligosaccharides	S-5
Figure S2. Structures of the glycolipids	S-6
Figure S3. ESI-MS analysis of picodiscs.....	S-8
(a) <i>Library 1</i>	S-8
(b) <i>Library 2</i>	S-8
(c) <i>Library 3</i>	S-8

(d) <i>Library 4</i>	S-8
Figure S4. CID mass spectra of <i>Library 1</i> and <i>Library 2</i>	S-9
(a) <i>Library 1</i> at collision energies (in Trap) of 30 V	S-9
(b) <i>Library 1</i> at collision energies (in Trap) of 50 V	S-9
(c) <i>Library 1</i> at collision energies (in Trap) of 100 V	S-9
(d) <i>Library 2</i> at collision energies (in Trap) of 30 V	S-9
(e) <i>Library 2</i> at collision energies (in Trap) of 50 V	S-9
(f) <i>Library 2</i> at collision energies (in Trap) of 100 V	S-9
Figure S5. ESI-MS analysis of nanodiscs	S-10
(a) ESI-MS spectrum of 2% 7G nanodiscs	S-10
(b) CID mass spectrum of the 2% 7G nanodiscs.....	S-10
Figure S6. CID mass spectra of CTB₅ with GD1a/b picodiscs	S-11
(a) CID mass spectrum of CTB ₅ with GD1a picodiscs	S-11
(b) CID mass spectrum of CTB ₅ with GD1b picodiscs	S-11
Figure S7. ESI-MS analysis of Stx1-B₅ with <i>Library 2</i>	S-12
(a) ESI-MS spectrum of Stx1-B ₅ with <i>Library 2</i>	S-12
(b) CID mass spectrum of the (Stx1-B ₅ + L) ¹¹⁻ ion	S-12
Figure S8. ESI-MS analysis of CTB₅ with ganglioside oligosaccharides	S-13
(a) ESI-MS spectrum of CTB ₅ with GM2 _{os}	S-13
(b) ESI-MS spectrum of CTB ₅ with GM3 _{os}	S-13
(c) ESI-MS spectrum of CTB ₅ with GD1a _{os}	S-13
(d) ESI-MS spectrum of CTB ₅ with GD1b _{os}	S-14
(e) ESI-MS spectrum of CTB ₅ with GD2 _{os}	S-14
(f) ESI-MS spectrum of CTB ₅ with GT1b _{os}	S-14
Figure S9. Titration curves of CTB₅ with ganglioside oligosaccharides	S-15
(a) Titration curve of CTB ₅ with GM2 _{os}	S-15
(b) Titration curve of CTB ₅ with GM3 _{os}	S-15
(c) Titration curve of CTB ₅ with GD1a _{os}	S-15
(d) Titration curve of CTB ₅ with GD1b _{os}	S-16
(e) Titration curve of CTB ₅ with GT1b _{os}	S-16
Figure S10. CID mass spectra of TcdA-A2 with GD1a/b picodiscs	S-17

(a) CID mass spectrum of TcdA-A2 with GD1a picodiscs.....	S-17
(b) CID mass spectrum of TcdA-A2 with GD1b picodiscs	S-17
Figure S11. CID mass spectra of the L_{a1}^- and L_{b1}^- ions.....	S-18
(a) CID mass spectrum of the L_{a1}^- ion	S-18
(b) CID mass spectrum of the L_{b1}^- ion	S-18
(c) Fragmentation scheme shown for L_{a1}^-	S-18
Figure S12. CID mass spectra of the L_{a2}^-, L_{b2}^-, L_{c2}^- and L_{d2}^- ions	S-19
(a) CID mass spectrum of the L_{a2}^- ion	S-19
(b) CID mass spectrum of the L_{b2}^- ion	S-19
(c) CID mass spectrum of the L_{c2}^- ion	S-19
(d) CID mass spectrum of the L_{d2}^- ion	S-19
(e) Fragmentation scheme shown for L_{a2}^-	S-19

Table S1. Composition of lipids (phospholipid and glycosphingolipid) in *Library 1*, *Library 2*, *Library 3* and *Library 4*, which were used to produce the picodiscs.

Library	Phospholipid	Glycolipids
<i>Library 1</i>	POPC	GM1, GM2, GM3, GD2, GD1a, GD1b and GT1b
<i>Library 2</i>	POPC	GM1, GM2, GM3, GD2, GD1a, GD1b and GT1b
<i>Library 3</i>	POPC	Glycolipids extract from porcine brain
<i>Library 4</i>	POPC	Glycolipids extract from cultured human epithelial A549 cell line

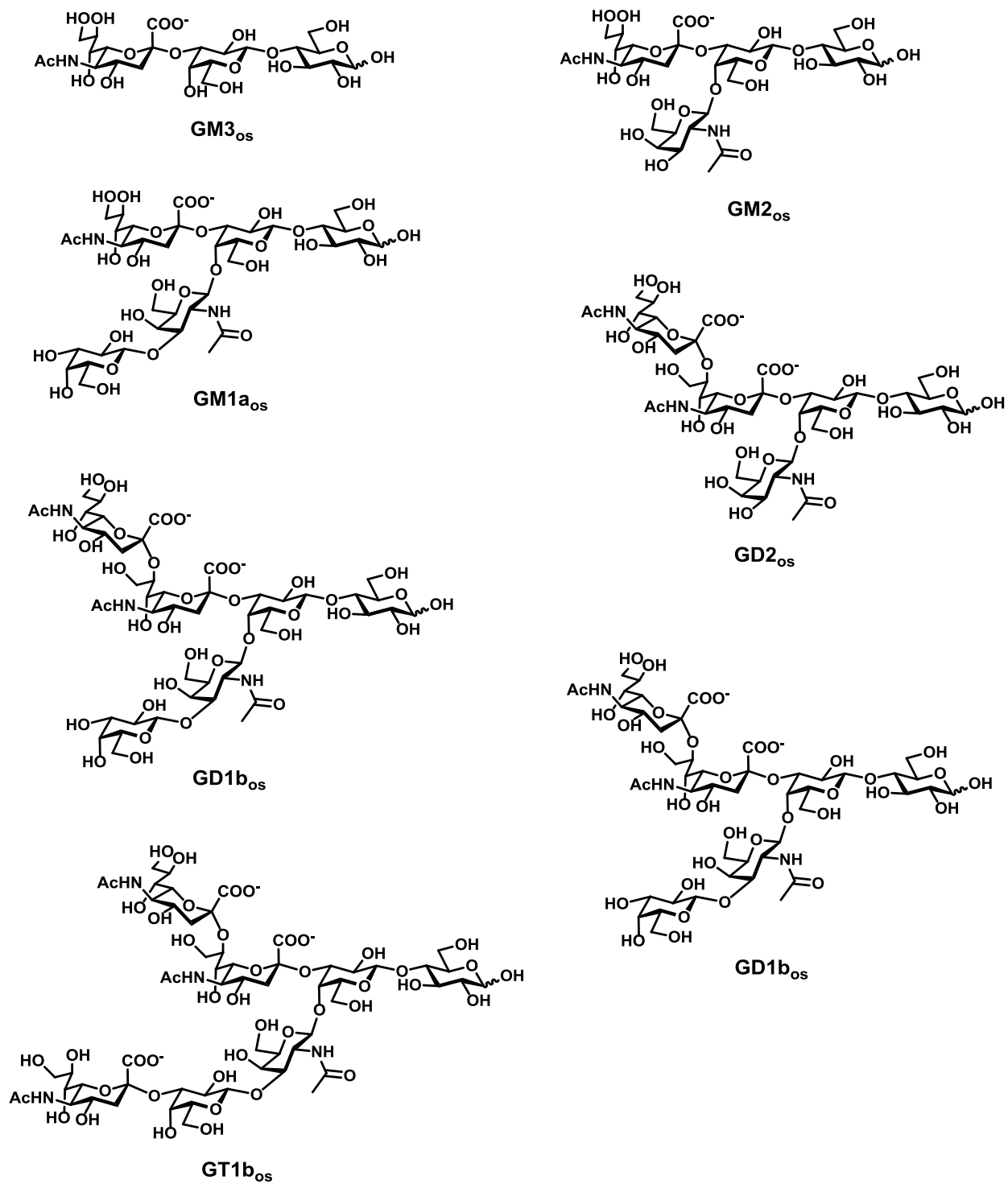
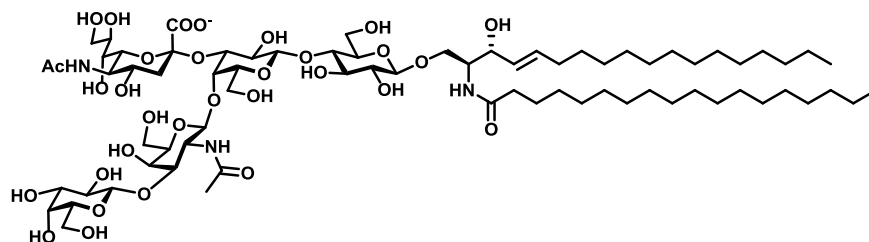
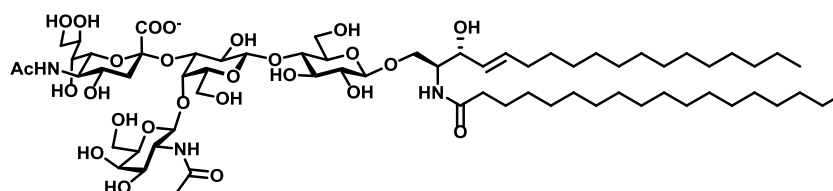


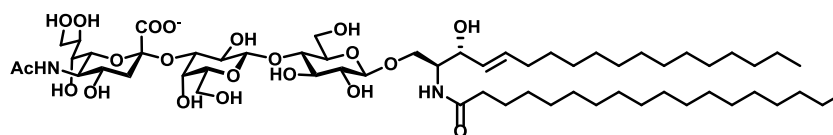
Figure S1. Structures of the ganglioside oligosaccharides GM3_{os}, GM2_{os}, GD2_{os}, GD1a_{os}, GD1b_{os} and GT1b_{os}.



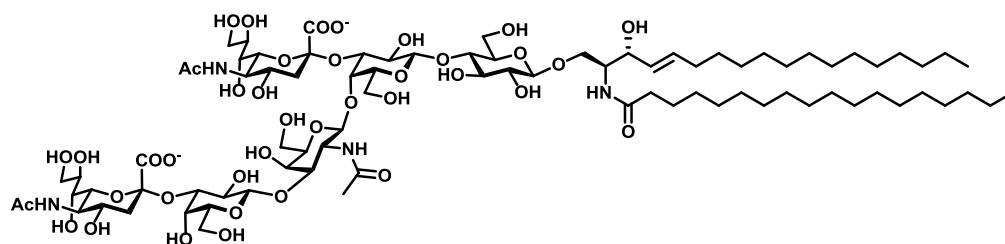
d18:1-18:0
GM1



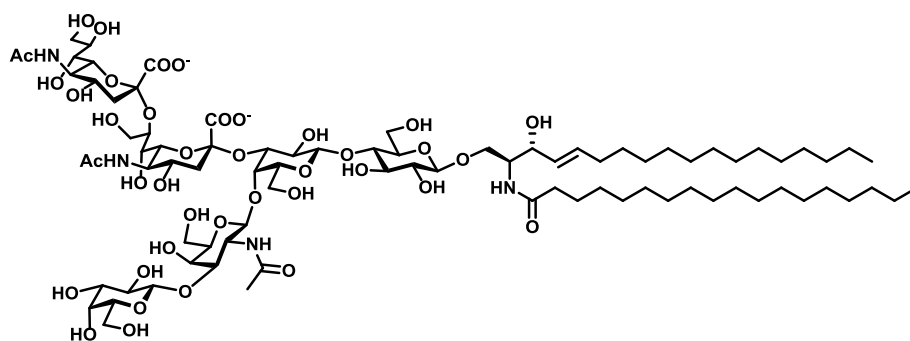
d18:1-18:0
GM2



d18:1-18:0
GM3



d18:1-18:0
GD1a



d18:1-18:0
GD1b

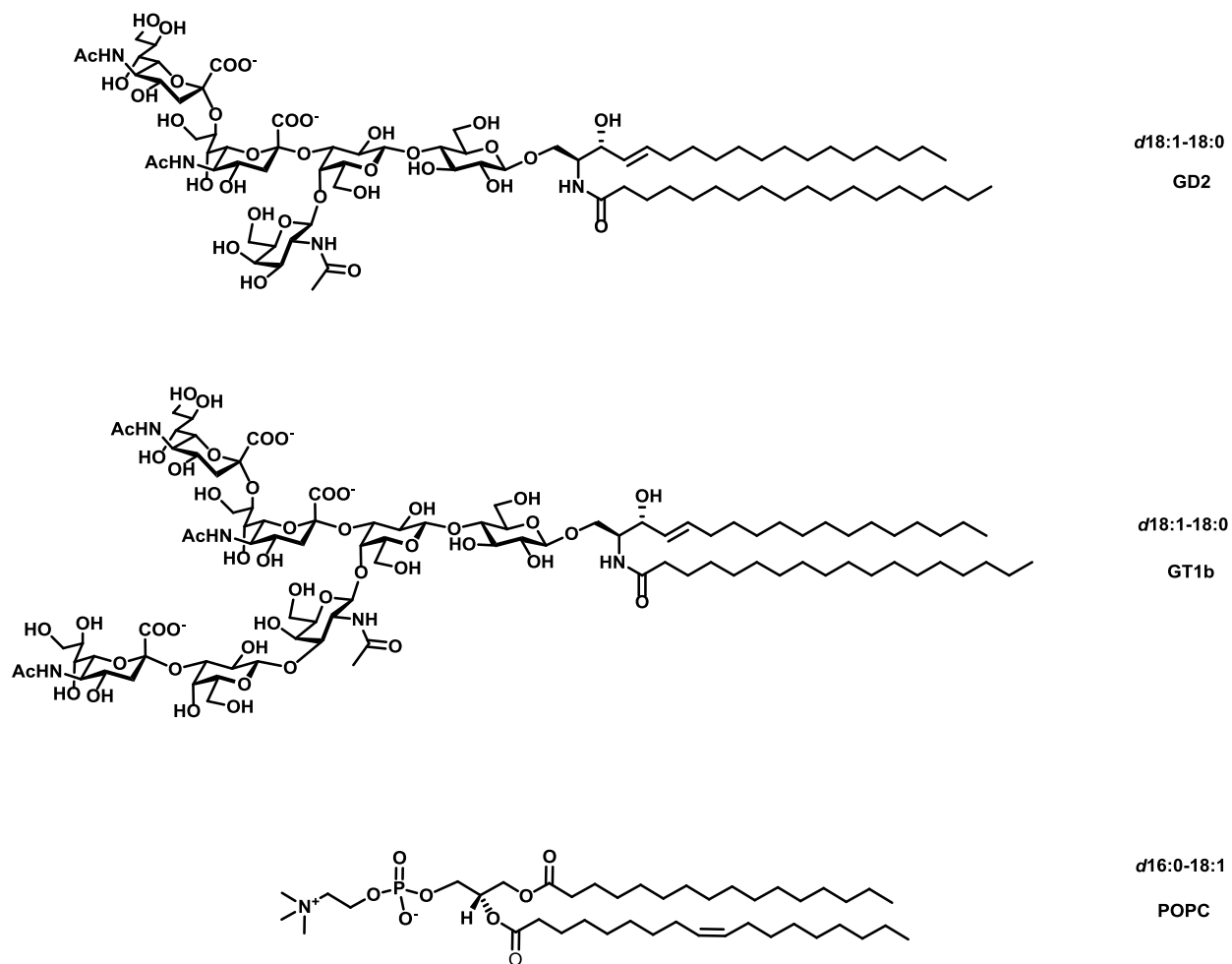


Figure S2. Structures of the gangliosides GM1, GM2, GM3, GD2, GD1a, GD1b and GT1b and the phospholipid POPC.

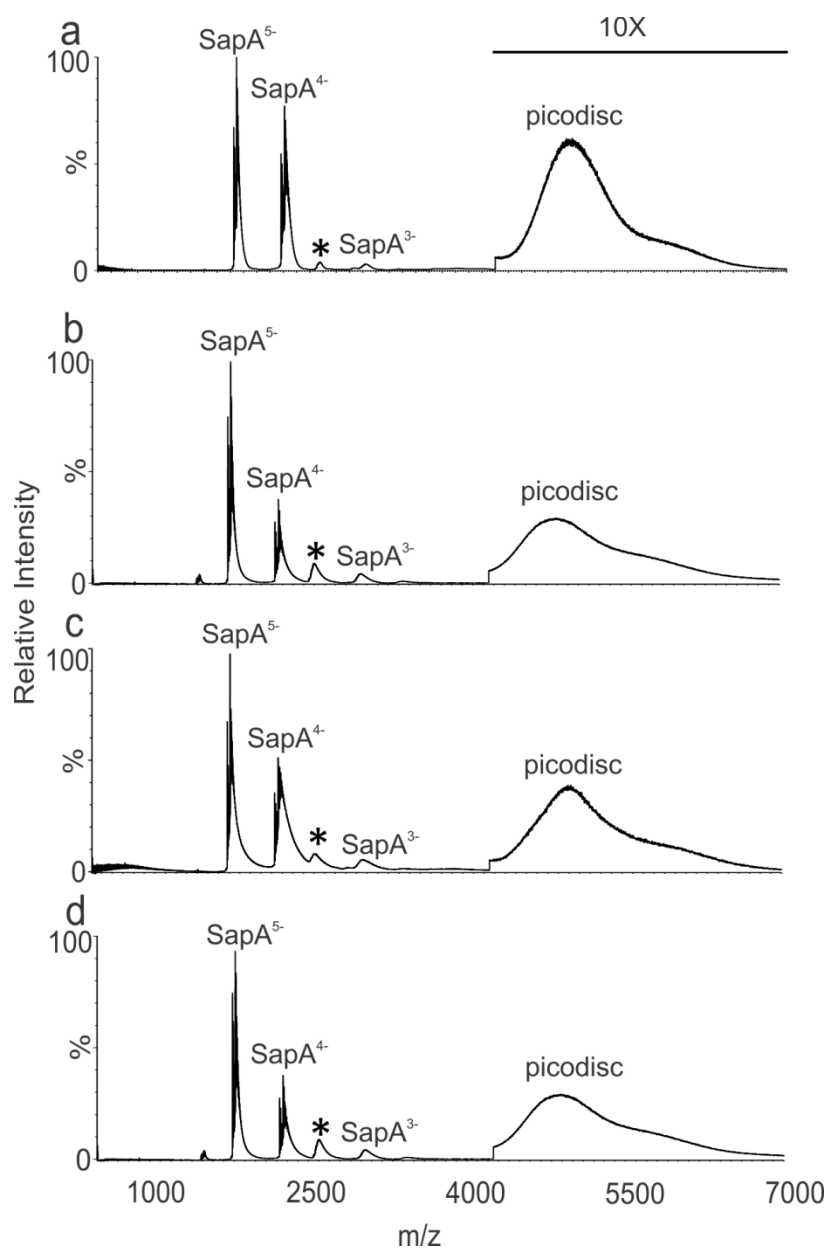


Figure S3. ESI mass spectra acquired in negative ion mode for aqueous ammonium acetate solutions (200 mM, pH 6.8) of (a) *Library 1* (20 μ M of each PD), (b) *Library 2* (140 μ M), (c) *Library 3* (40 μ M) and (d) *Library 4* (140 μ M). Peaks labelled * correspond to (SapA + POPC) complexes.

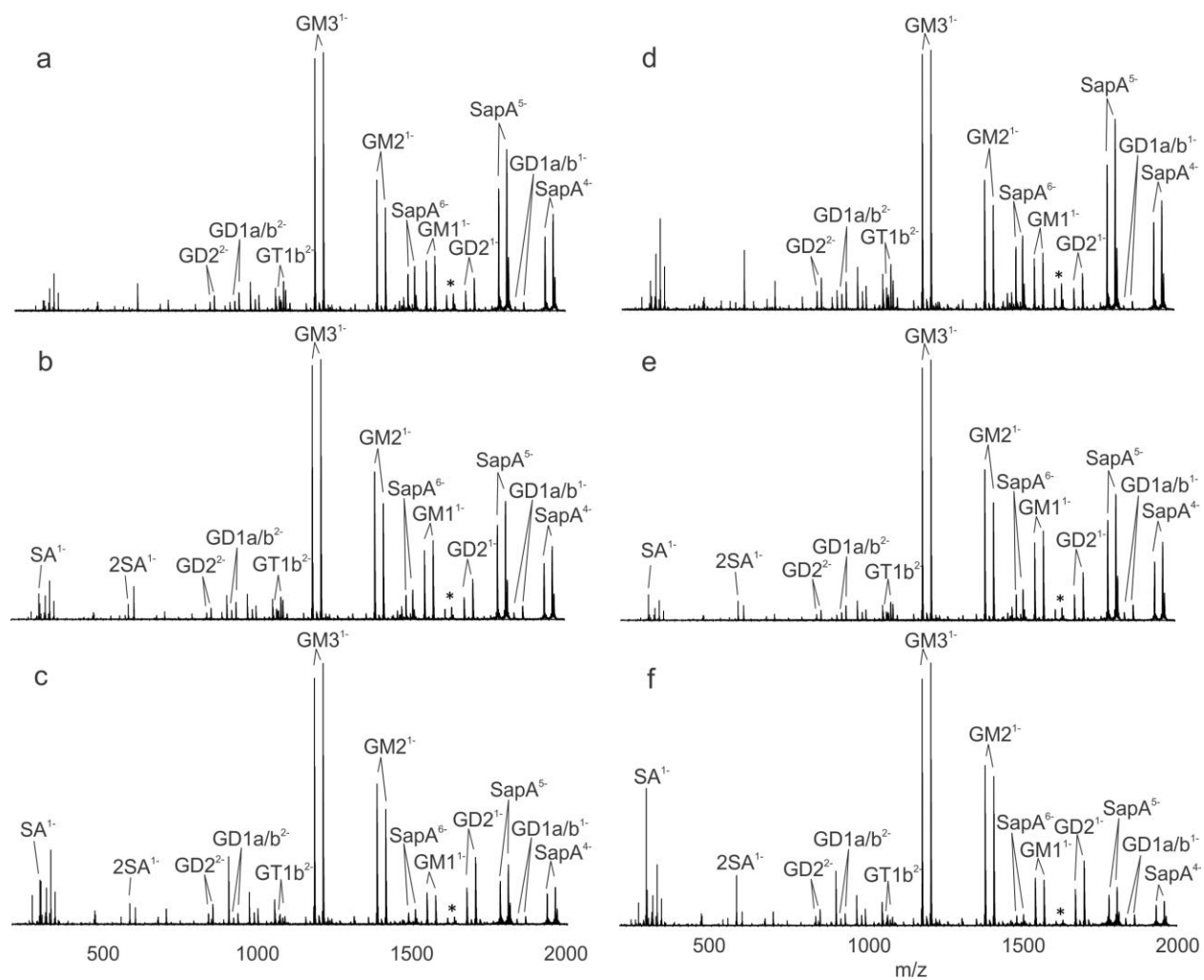


Figure S4. CID mass spectra of ions with $m/z > 4000$, produced by ESI performed in negative ion mode on aqueous ammonium acetate solutions (200 mM, pH 6.8) of *Library 1* (20 μ M each PD), at collision energies (in Trap) of (a) 30 V, (b) 50 V and (c) 100 V, and of *Library 2* (140 μ M) at collision energies (in Trap) of (d) 30 V, (e) 50 V, and (f) 100 V. Peaks labelled * correspond to (SapA + POPC) complexes.

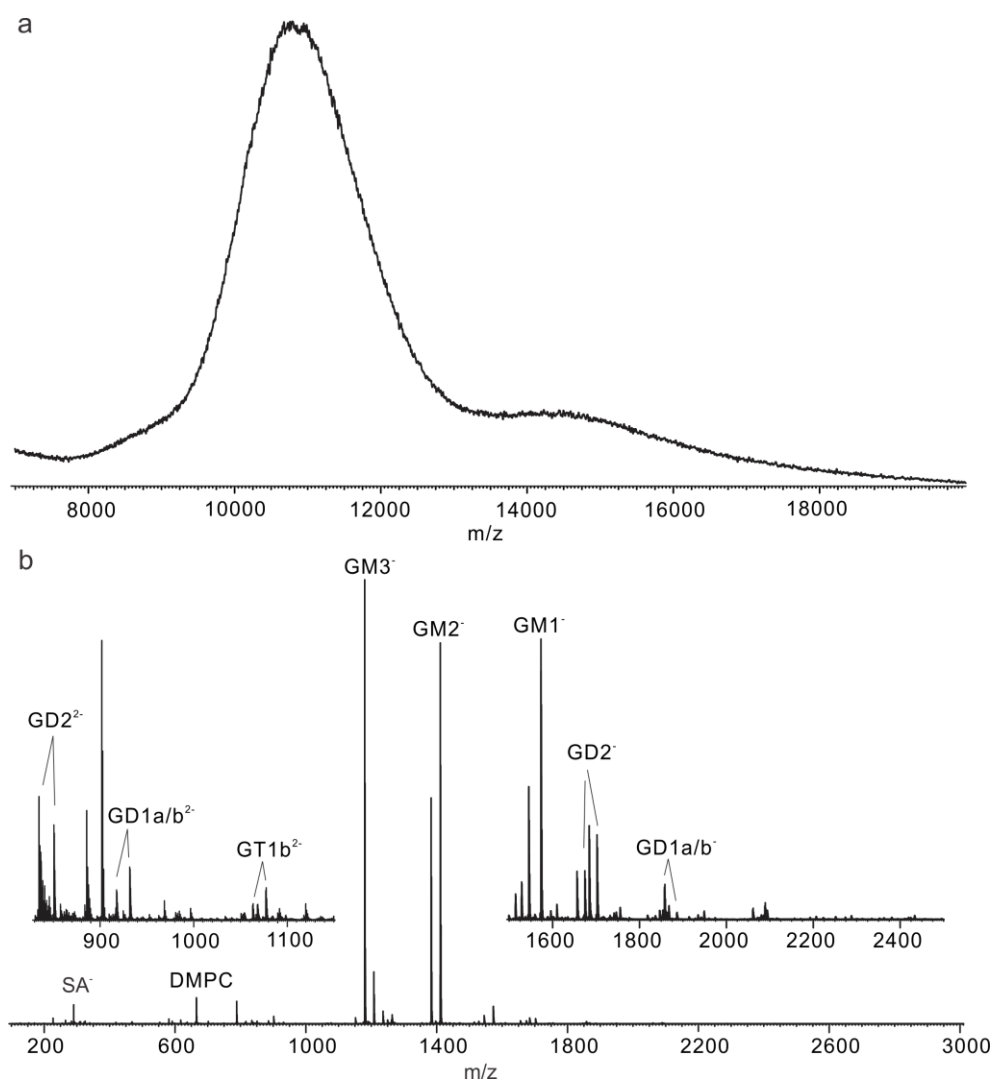


Figure S5 (a) ESI mass spectrum acquired in negative ion mode for an aqueous ammonium acetate solution (200 mM, pH 6.8) of 7G ND (6 μ M, 2% of each ganglioside). (b) CID mass spectrum of ions with $m/z > 5600$, produced by ESI for the solution described in (a), using a collision energy (in Trap) of 150 V.

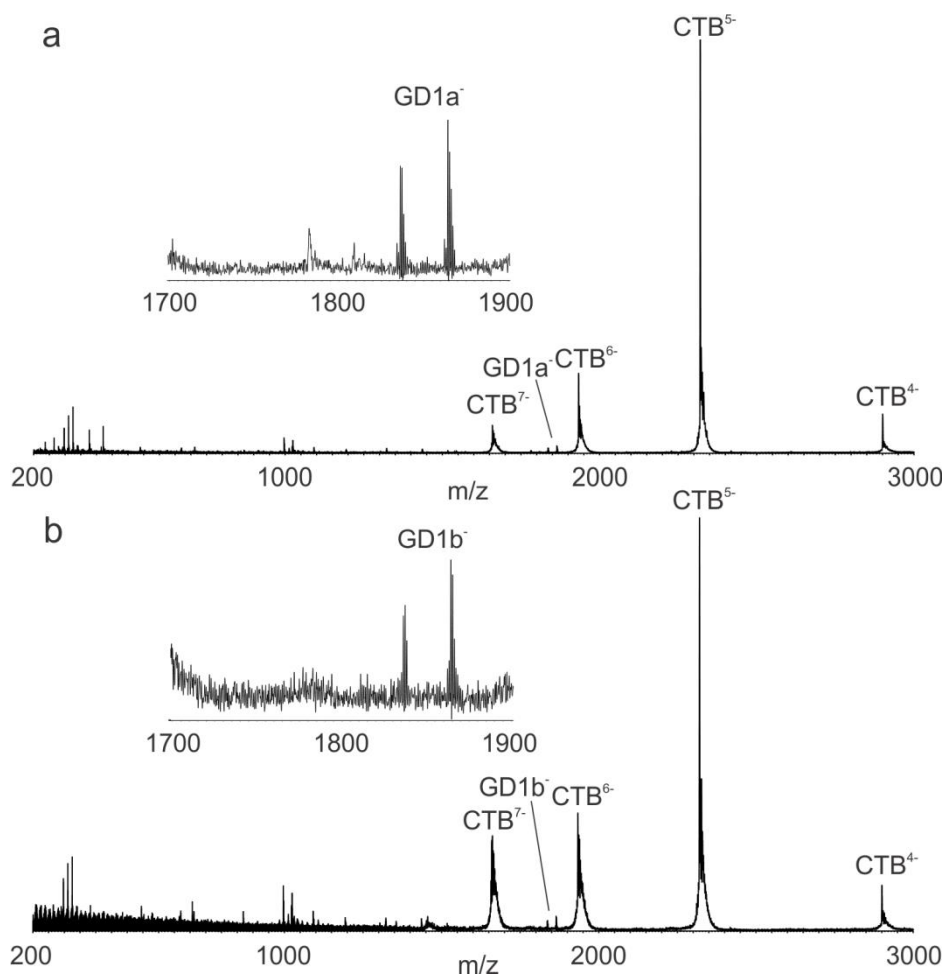


Figure S6 CID mass spectra of free and any ligand-bound CTB₅ ions, at charge states -12 to -15, produced in negative ion mode by ESI performed on an aqueous ammonium acetate solutions (200 mM, pH 6.8) containing CTB₅ (3 μM) and 6 μM of (a) GD1a PD or (b) GD1b PD. CID was performed with a collision energy of 75 V in the Transfer region following IMS separation of CTB₅ ions from the PD ions.

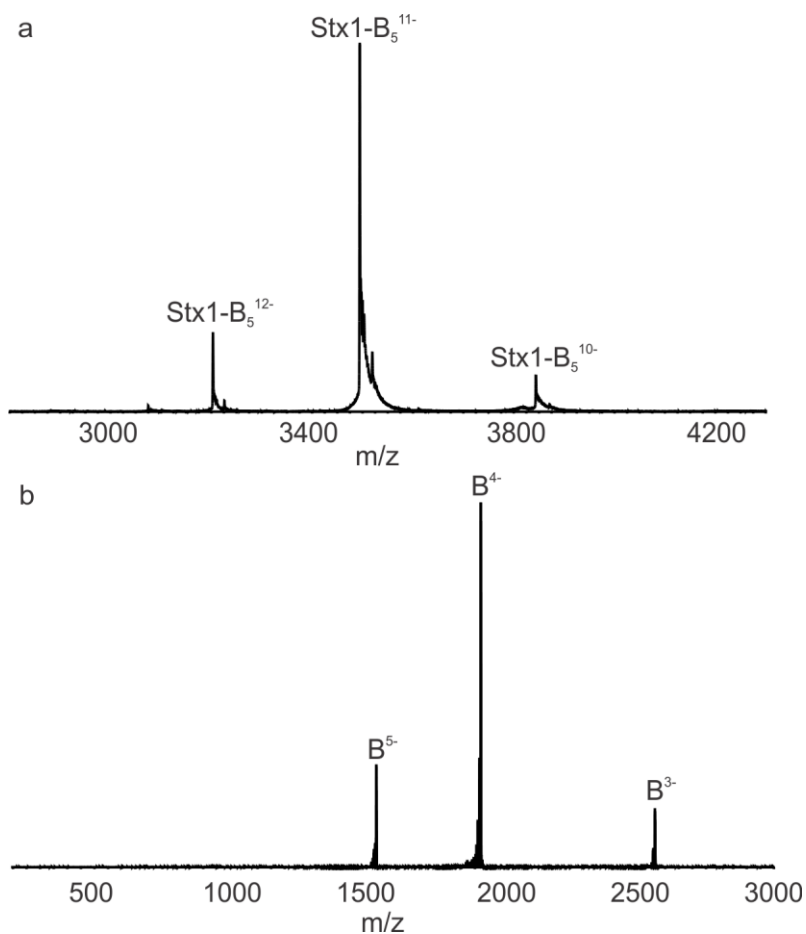
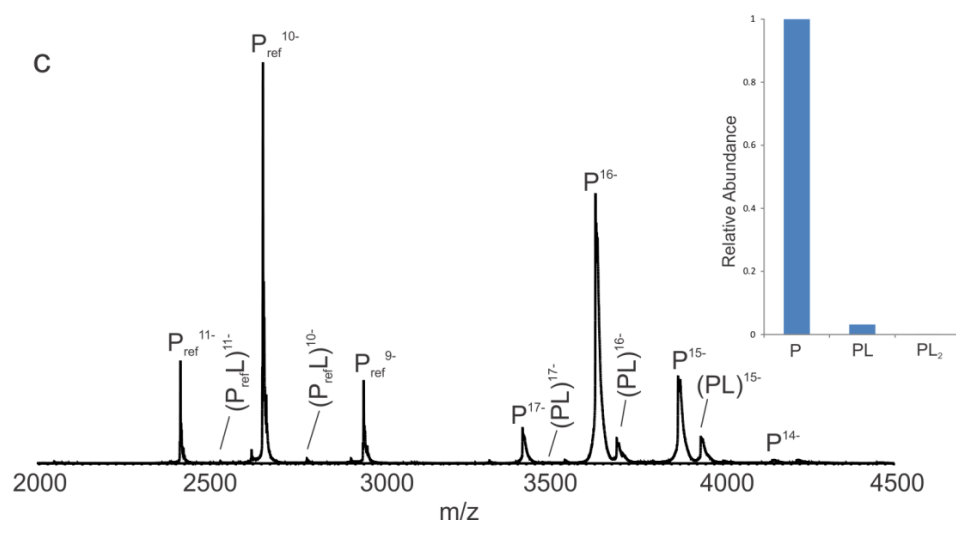
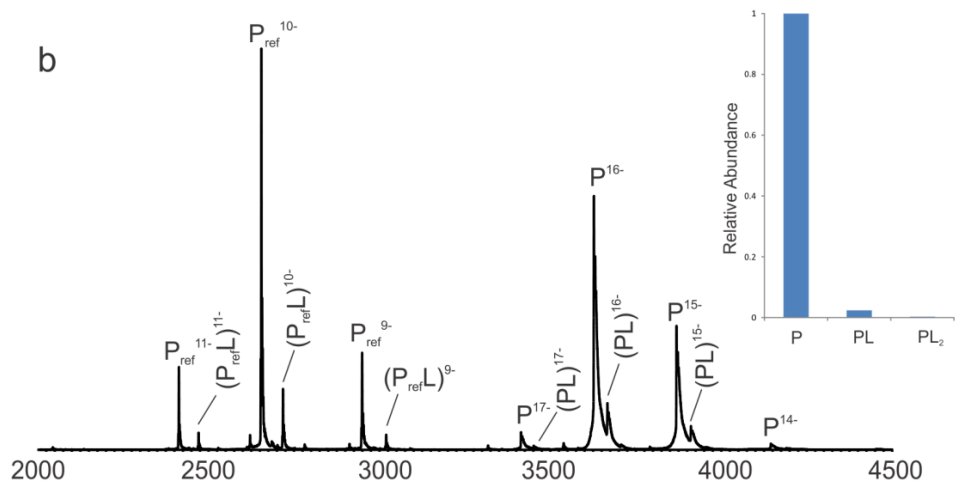
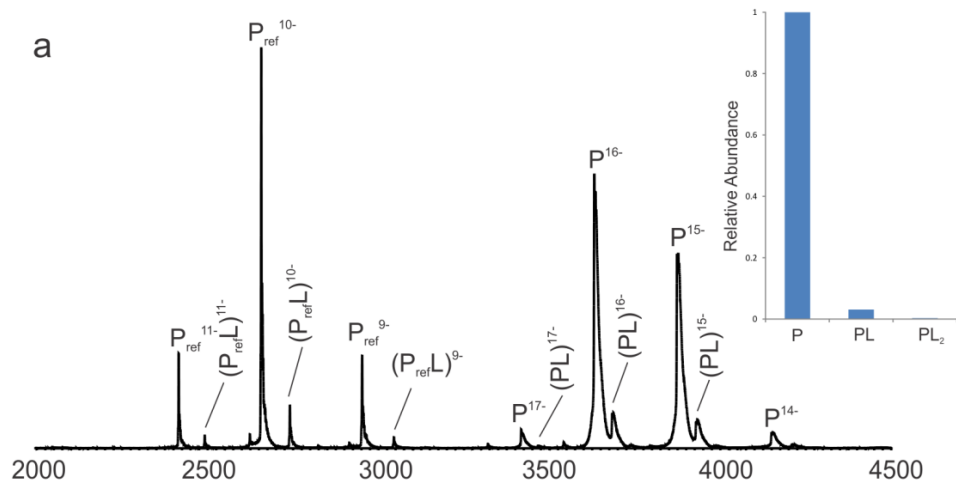


Figure S7. (a) ESI mass spectrum acquired in negative ion mode for an aqueous ammonium acetate solution (200 mM, pH 6.8) of Stx1-B₅ (5 μM) and *Library 2* (56 μM). (b) CID mass spectrum acquired in the Trap region on possible (Stx1-B₅ + L)¹¹⁻ ions using a collision energy of 50 V.



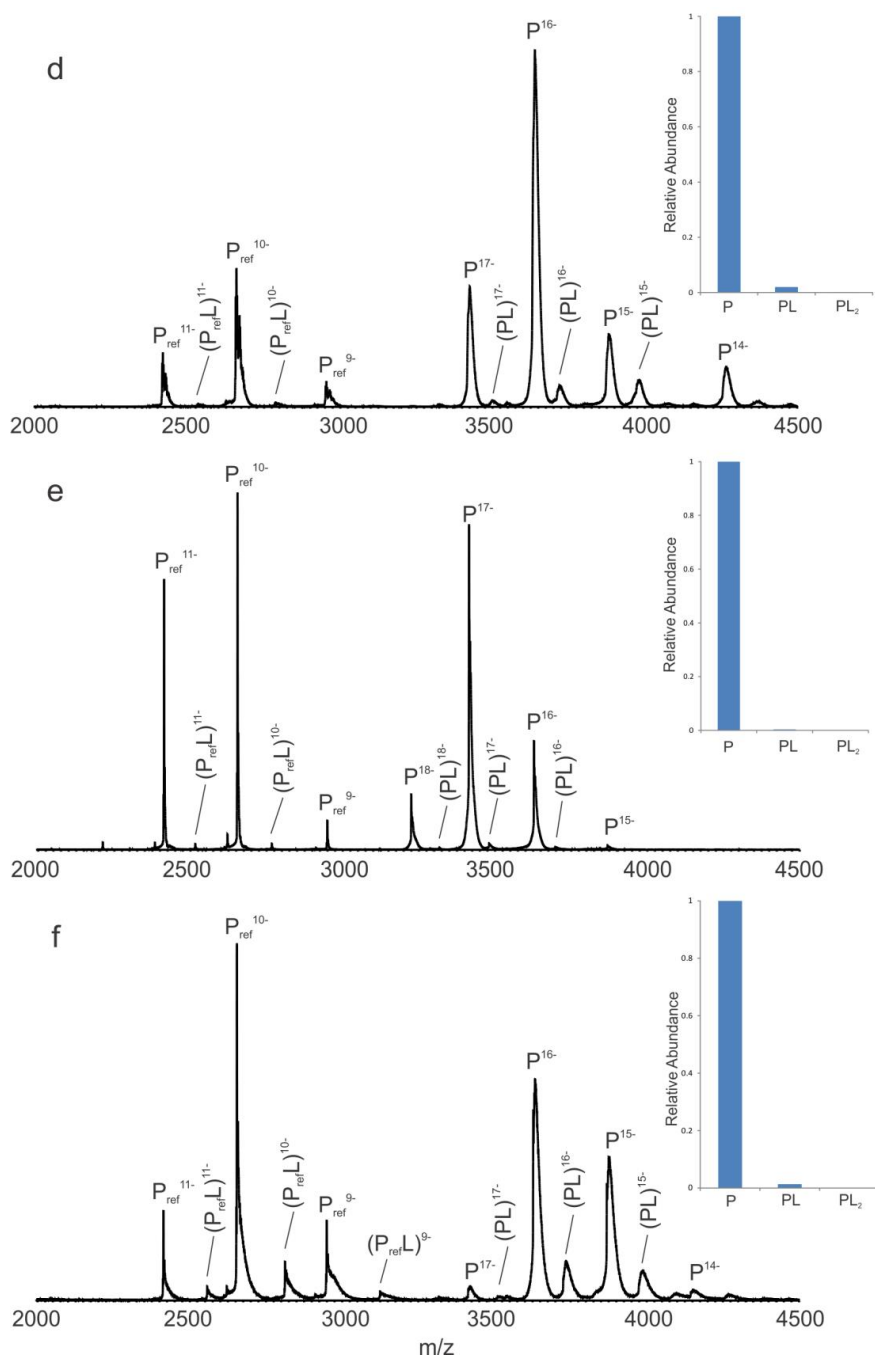
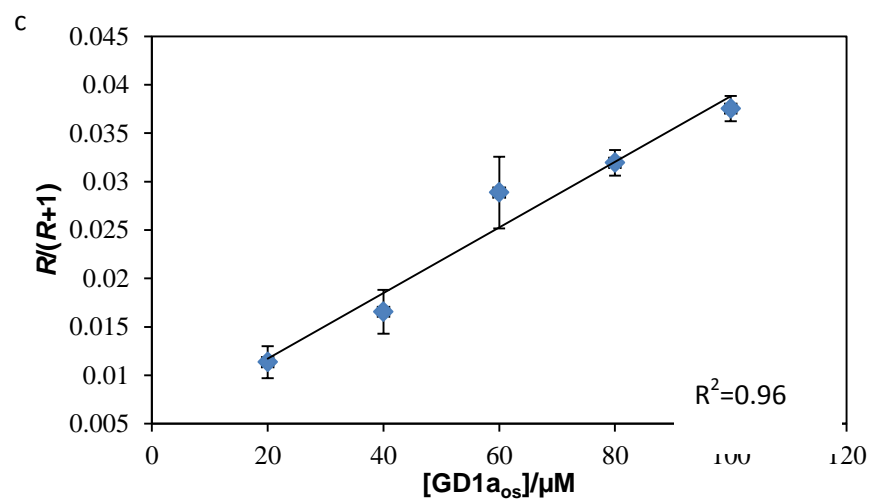
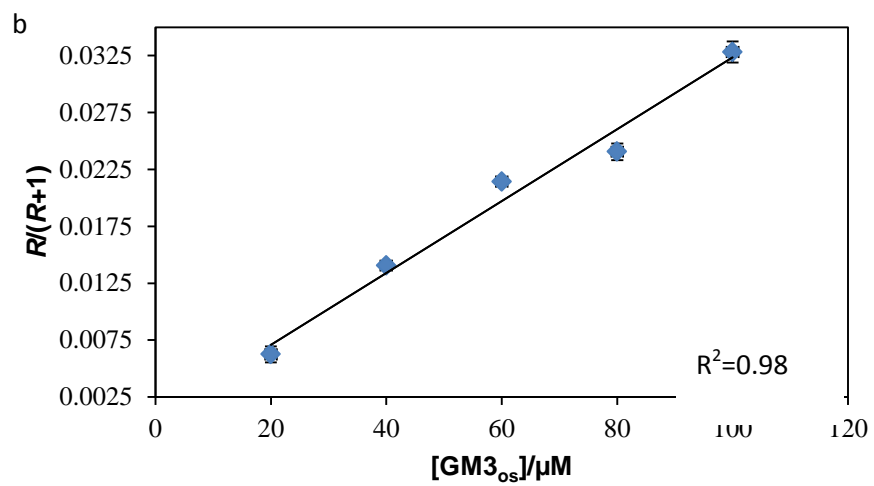
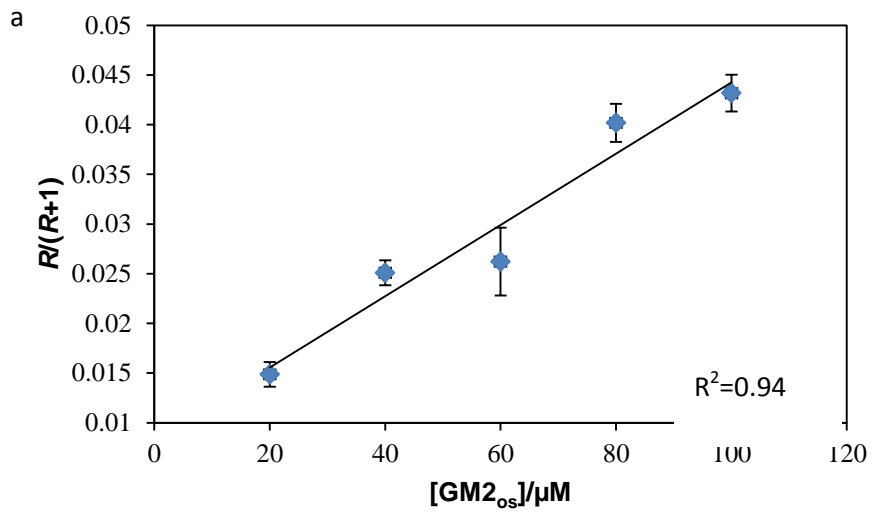


Figure S8. ESI mass spectra acquired in positive ion mode for aqueous ammonium acetate solutions (200 mM, pH 6.8) of CTB₅ (6 μM), P_{ref} (2 μM), and the ganglioside oligosaccharide (60 μM) (a) GM2_{os}, (b) GM3_{os}, (c) GD1a_{os}, (d) GD1b_{os}, (e) GD2_{os} or (f) GT1b_{os}. Insets show the normalized distributions of free and ligand-bound forms of CTB₅.



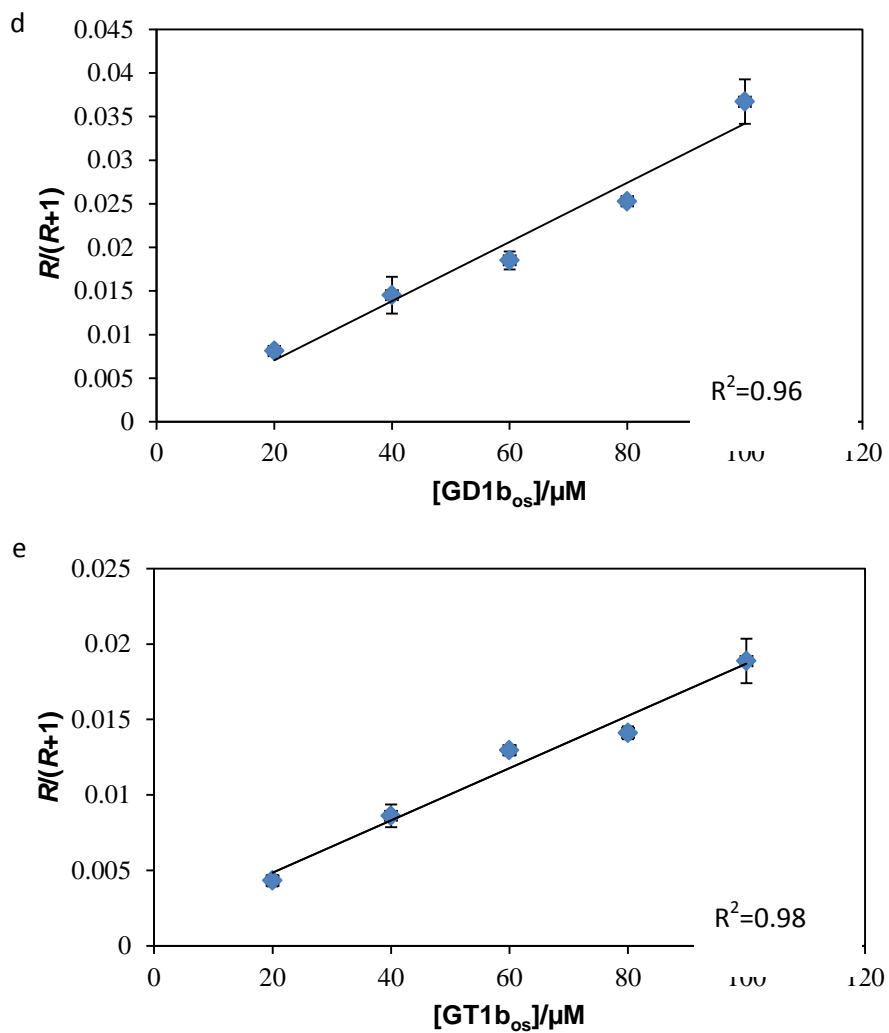


Figure S9. Plot of the fraction of ligand-bound CTB₅ (i.e., $R/(R+1)$) versus ligand concentration measured for the ganglioside oligosaccharides (a) GM2_{os}, (b) GM3_{os}, (c) GD1a_{os}, (d) GD1b_{os} and (e) GT1b_{os}. The concentration of CTB₅ was fixed at 6 μM and the concentration of oligosaccharide varied from 0 to 100 μM . The error bars correspond to one standard derivation.

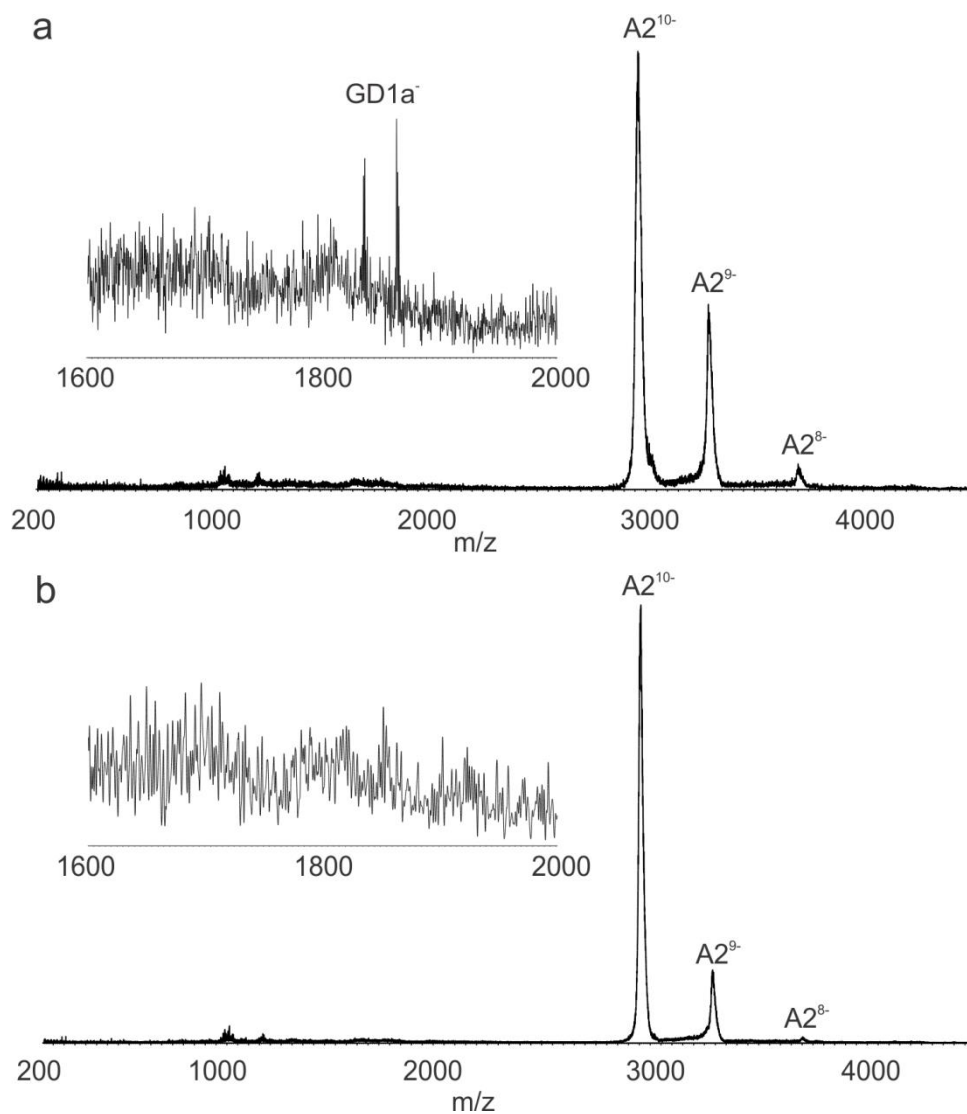


Figure S10 CID mass spectra acquired for ions with m/z between 2944 and 3344 produced by ESI performed in negative ion mode on aqueous ammonium acetate solutions (200 mM, pH 6.8) of TcdA-A2 (6 μ M) and (a) GD1a PD (17 μ M) or (b) GD1b PD (17 μ M). CID was performed in the Trap region using a collision energy of 50 V.

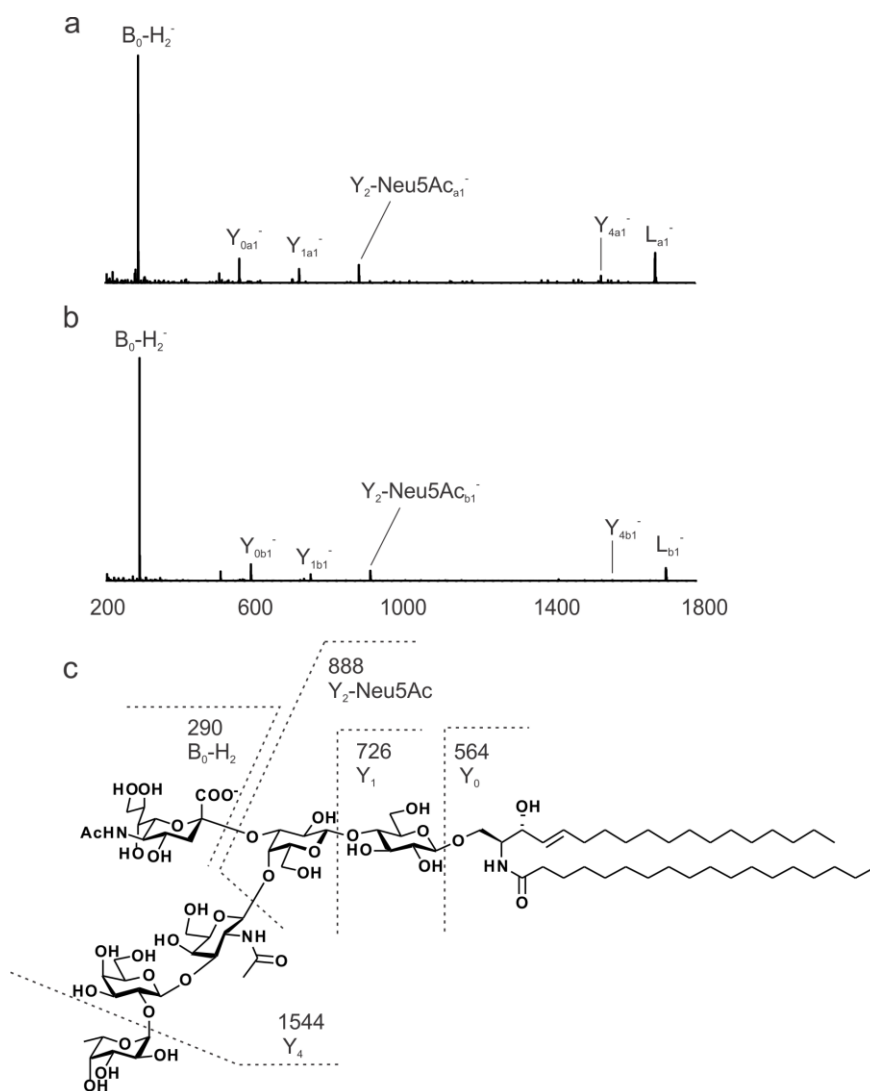


Figure S11. CID mass spectra acquired for (a) the L_{a1}^- ion (m/z 1690.8) or (b) the L_{b1}^- ion (m/z 1718.8), produced by ESI performed in negative ion mode on a methanol solution of *Library 3*. $B_0-H_2^-$ corresponds to deprotonated 5-N-acetyl-neuraminic acid (Neu5Ac); Y_{4a1}^- and Y_{4b1}^- result from loss of the fucosyl moiety from L_{a1}^- and L_{b1}^- , respectively; $Y_2-Neu5Ac_{a1}^-$ and $Y_2-Neu5Ac_{b1}^-$ result from loss of the Fuc, Gal, GalNAc and Neu5Ac residues from L_{a1}^- and L_{b1}^- , respectively; Y_{1a1}^- and Y_{1b1}^- result from the loss of Gal residue from $Y_2-NeuAc_{a1}^-$ and $Y_2-NeuAc_{b1}^-$, respectively; and Y_{0a1}^- and Y_{0b1}^- result from the loss of Glc residue from Y_{1a1}^- and Y_{1b1}^- , respectively. (c) Fragmentation scheme shown for L_{a1}^- (*d* 18:1-18:0).

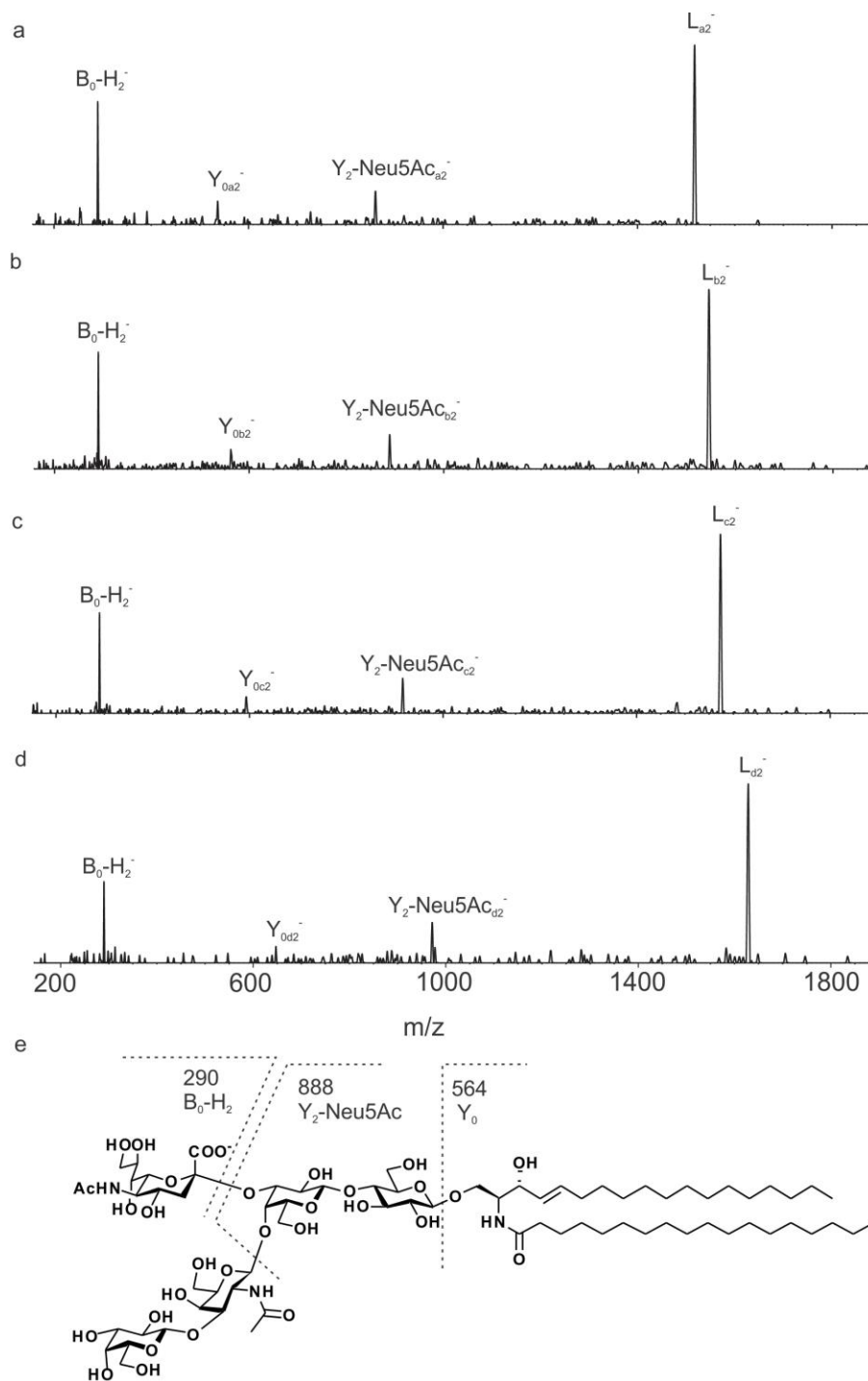


Figure S12. CID mass spectra acquired for the (a) the L_{a2}^- (at m/z 1517.0), (b) L_{b2}^- (at m/z 1545.1), (c) L_{c2}^- (at m/z 1573.1) and (d) L_{d2}^- (at m/z 1629.1) ion, produced by ESI performed in negative ion mode on a methanol solution of *Library 4*. $B_0-H_2^-$ corresponds to deprotonated Neu5Ac; $Y_2-Neu5Ac_{a2}^-$, $Y_2-Neu5Ac_{b2}^-$, $Y_2-Neu5Ac_{c2}^-$ and $Y_2-Neu5Ac_{d2}^-$ result from loss of the

Gal, GalNAc and Neu5Ac residues from L_{a2}^- , L_{b2}^- , L_{c2}^- and L_{d2}^- , respectively; Y_{0a2}^- , Y_{0b2}^- , Y_{0c2}^- and Y_{0d2}^- result from the loss of Gal and Glc residues from Y_2 -NeuAc $_{a2}^-$ and Y_2 -NeuAc $_{b2}^-$, Y_2 -NeuAc $_{c2}^-$ and Y_2 -NeuAc $_{d2}^-$, respectively. (e) Fragmentation scheme shown for L_{a2}^- (*d*18:1-18:0).